Constructive geometry / root iterations / global convergence

# Geometric Root Calculators

Radical supports of orders five and nine and real-degree enclosures in the Pandrosion rectangle

Ivan Besevic[1] · Independent research
Version 29 (revision of V28) · 13 November 2026
https://github.com/ivan-fr/pandrosion

**Abstract.** We study ruler-and-compass iterations for the positive root $X^{1/p}$ that share one rectangle, one power stage and one readout, and differ only in a *support line*. Every support approximates the same target function $\kappa_*(t) = (t-1)/(t^{1/p}-1)$ of the residual $t$, and the contact order of the approximation fixes the order of the iteration. Besides the classical supports of orders one to four we treat three radical supports. A decentered arc gives a globally monotone fifth-order iteration. Two supports have local order *exactly nine for every real* $p > 2$ and converge monotonically from every positive start: a support built from two successive mean proportionals, with error constant $7/648$ for cube roots, and a combination of the arithmetic mean, the geometric mean and one conic mean of 1 and $t$, with error constant $23/20736$ for cube roots, drawn with three arcs. For integer $p \geq 3$ one step costs at most $10p+9$ elementary traces for the decentered arc, $10p+11$ for the three-mean support and $10p+59$ for the nested support; measured by the efficiency index, and under the stated counting conventions, the three-mean support is preferable for every $p \geq 3$. We then separate what is a finite construction from what is only a scalar statement: the fast iterations are finite constructions for rational degrees, whereas for irrational $p$ a single step is not. For arbitrary real $p \neq 0$ a power-free subdivision with one final Padé readout encloses the root with relative width at most $z^5/256$ in at most $15n+63$ traces after $n$ subdivisions (for $X > 1$, $p \geq 1$). Global convergence and the local orders with their constants, for the three radical supports and every real $p > 2$, are checked in Lean, as are the degree, approximation and efficiency statements; the drawing inventories are written protocols.

hexagon:2611.00495v1

## 1 Introduction

A geometric iteration must realize its arithmetic by intersections, parallels and length transfers. The Pandrosion rectangle does this for $p$th roots: a chain of similar triangles produces the power $s^p$ of the current estimate, a line through a prepared point transports the residual, and a horizontal reads the next estimate on the same rail. The only part that changes from one method to another is the *support*, a line through the corner $A$ whose slope encodes a correction factor.

**Results.**

1. **One target function** (Section 2). All supports approximate $\kappa_*(t) = (t-1)/(t^{1/p}-1)$; contact of order $\omega$ at $t = 1$ gives an iteration of order $\omega+1$ with an explicit error constant (Lemma 2.1). Newton, Halley and the [1/1] Padé support are the cases $\omega = 1, 2, 3$.
2. **Decentered arc** (Section 3). One moving arc and one join give $\omega = 4$: a fifth-order iteration, monotone and convergent from every positive start for real $p > 2$ (Theorem 3.1).
3. **Nested radicals** (Section 4). Two successive mean proportionals give $\omega = 8$. The iteration has order exactly nine for every real $p > 2$, with the closed-form constant of Theorem 4.1; it is globally monotone (Theorem 4.4).
4. **Three means** (Section 5). A combination of the arithmetic mean, the geometric mean and one conic mean of 1 and $t$ also gives $\omega = 8$. It is drawn with three arcs and one join, has order exactly nine with a smaller constant, and is globally monotone (Theorem 5.1).
5. **Work** (Section 6). Per-step inventories of the nested and three-mean supports (Propositions 6.1 and 6.2), a comparison of seven supports at a common state, and an efficiency-index comparison

[1]Computational assistance: the AI systems ChatGPT (OpenAI) and Claude (Anthropic) were used for derivations, proof development, figures and manuscript preparation. The author is responsible for the claims and their attribution. Section 9 states, claim by claim, which results are formal proofs, written proofs, computer-algebra identities or numerical checks.

(Proposition 6.3): the nested support overtakes the decentered arc at $p = 13$, and the three-mean support has the largest index for every $p \geq 3$.

6. **Degrees** (Sections 4.5 and 7). A classification of what is constructible in finitely many traces per step, summarized in Table 1, and a direct enclosure for every real $p \neq 0$ (Propositions 7.1 and 7.2).

**Table 1:** Which calculator applies to which degree. "Finite step" means that one iteration step is a finite ruler-and-compass construction from the current state.

| Degree $p$ | Fast rectangle iterations (orders 2–9) | Direct subdivision (Section 7) |
|---|---|---|
| Integer $p \geq 3$ | Finite step; $10p+9$, $10p+11$ or $10p+59$ traces | Yes |
| Rational $p = \mu/\nu$ | Finite step, as degree $\mu$ applied to $X^\nu$ (Proposition 4.5) | Yes |
| Irrational $p$ | Step not finite: $u^p$ is itself a real power. Available only through a rational approximation of $p$ (Proposition 4.7) | Yes; this is the recommended route |

**What "construct" means here.** As in Pandrosion's recursive geometry, nothing in this paper constructs $X^{1/p}$ exactly in finitely many operations; $\sqrt[3]{2}$ is not constructible. A calculator is a rule whose every step is a finite construction and whose successive outputs converge to the root, with a stated rate or a stated enclosure. The distinction that matters is therefore not exact versus approximate, but whether *each step* is finite. Scalar convergence theorems are stated for real $p$; drawing inventories are stated only where a step is a finite construction.

**Relation to earlier versions.** The classical supports and the decentered arc were introduced in the earlier preprint [22]; they are restated here with complete proofs so that the comparison is self-contained. New in the present line of versions are the nested-radical support and its inventory. V28 added the contact lemma, the general ninth-order constant, the efficiency-index comparison, and the degree classification of Table 1 with the rational and irrational cases treated separately. New in this revision is the three-mean support of Section 5, with its Lean proofs, its construction and its inventory; the comparisons of Section 6 are updated accordingly. The linear baseline, called MA in earlier versions, is renamed MB after its support line $MB$ (Appendix B). Limits of the results are collected once, in Section 10.

# 2 Coordinates, arithmetic and the common support equation

## 2.1 States and notation

For $X > 0$ and $p \neq 0$ let $r = X^{1/p}$ be the root and $\alpha = 1/r$ its reciprocal. The rectangle carries a *reciprocal state* $s > 0$ approaching $\alpha$; the *direct state* is $u = 1/s$. The *residual* is

$$t = Xs^p = X/u^p, \qquad t = 1 \iff s = \alpha.$$

The logarithmic error is $e = \log(s/\alpha)$, so that $t = e^{pe}$. An iteration is written $s_+ = s\,\Phi(t)$. Table 2 fixes the main symbols.

## 2.2 Rectangle and line arithmetic

In the rectangle $C = (0,0)$, $B = (W,0)$, $O = (0,H)$, $A = (W,H)$, with $W, H > 0$, define

$$R(q) = (W, H(1-q)), \qquad L(q) = (0, H(1-q)), \qquad \Omega_f = \Big(\frac{Wf}{f-1}, H\Big) \quad (f \neq 1). \tag{2.1}$$

Line incidences perform multiplication and division:

$$\Omega_f R(q) \cap OC = L(fq), \qquad \Omega_f L(b) \cap AB = R(b/f). \tag{2.2}$$

Substituting the coordinates into the line equations proves both identities. Unit factors and zero values reuse existing points instead of a centre at infinity.

**Table 2:** Notation.

| | |
|---|---|
| $X,\ p,\ r,\ \alpha$ | input, degree, root $X^{1/p}$, reciprocal root $X^{-1/p}$ |
| $s,\ u,\ t,\ e$ | reciprocal state, direct state $1/s$, residual $Xs^p$, log error $\log(s/\alpha)$ |
| $h,\ \xi,\ x$ | $h = 1/p;\ \ \xi = t-1;\ \ x = \log t$ |
| $W, H;\ A, B, C, O$ | rectangle width and height; its corners (Section 2.2) |
| $R(q), L(q), \Omega_f$ | right-rail point, left-rail point, projection centre on the top line |
| $M, E, P, T$ | prepared point, power endpoint $R(s^p)$, state point $R(s)$, intersection on the support |
| $\kappa,\ \kappa_*$ | normalized support slope; exact slope $(t-1)/(t^h-1)$ |
| $\mathsf{j}, \mathsf{p}, \mathsf{c}$ | one join, one constructed parallel ($= 2\mathsf{j} + 3\mathsf{c}$), one compass arc |
| $q_5,\ q_9,\ q_M$ | normalized slopes $(\kappa-1)/(p-1)$ of the decentered, nested and three-mean supports |
| $m, g, n, d;\ \tau, \lambda$ | (Section 5 and its inventory only) coefficients of $q_M$; $\ \tau = \sqrt{t},\ \ \lambda = H/X$ |
| $a, b$ | generic positive rail values; in Section 7, the moving endpoints |
| $m, \lambda, z$ | (Section 7 only) mean proportional $\sqrt{ab}$, weight, gap $b/a - 1$ |
| $\omega$ | order of contact of a support with $\kappa_*$ at $t = 1$ |
| $\mu, \nu$ | numerator and denominator of a rational degree $p = \mu/\nu$ |

**Triangle power stage.** Let $B_j = (Ws^j, H(1-s^j)) \in OB$ and $L_j = L(s^j)$. Horizontals transfer between these points and the rails. The parallel to $L_1B$ through $B_j$ meets the left rail at $L_{j+1}$, since its ordinate there is $H(1-s^j)+H(1-s)s^j = H(1-s^{j+1})$. For integer $p$, repetition gives $E = R(s^p)$ with $2p-1$ parallels and the join $L_1B$.

**Products.** For positive rail values $a, b$ with $b \neq 1$, draw $V = CR(b) \cap OA = \Omega_{1/b}$ and project $R(a)$ successively through $\Omega_{1/2}$, $V$, $\Omega_{1/2}$, $\Omega_{1/4}$. By (2.2) the successive values are $L(a/2)$, $R(ab/2)$, $L(ab/4)$, $R(ab)$: a general product costs five joins. Division is symmetric: project $R(a)$ through $V$ to $L(a/b)$ and return through $\Omega_{1/2}, \Omega_{1/4}, \Omega_{1/2}$, with values $R(2a/b)$, $L(a/(2b))$, $R(a/b)$; again five joins. Multiplication by a *prepared* constant $d > 0$ uses the two centres $\Omega_{d/[2(1+d)]}$ and $\Omega_{1/[2(1+d)]}$ and costs two joins.

## 2.3 The common support equation and its target

Prepare $M = (0, H(1-X^{-1}))$. With $P = R(s)$ and $E = R(s^p)$, the line $ME$ has slope $\sigma = H(1-t)/(WX)$. Let a *support* be a line through $A$ of slope $H\kappa/(WX)$. The parallel to $ME$ through $P$ meets the support at $T$, and the horizontal through $T$ meets the right rail at $P_+ = R(s_+)$ with

$$s_+ = s\,\frac{\kappa}{\kappa - 1 + t}. \tag{2.3}$$

Indeed the two lines are $y - H = \frac{H\kappa}{WX}(x - W)$ and $y - H(1-s) = \sigma(x - W)$; eliminating $x$ gives $H - y = Hs\kappa/(\kappa - 1 + t)$. The update is exact, $s_+ = \alpha$, precisely when $\kappa/(\kappa - 1 + t) = t^{-h}$, that is when

$$\kappa = \kappa_*(t) := \frac{t-1}{t^h - 1} \qquad (\kappa_*(1) = p). \tag{2.4}$$

The function $\kappa_*$ is not constructible from $t$; every support below is a constructible approximation of it.

**Lemma 2.1** (Contact lemma; limit form formalized in Lean)**.** *Let $\kappa(t)$ be analytic and positive near $t = 1$ with $\kappa(t) - \kappa_*(t) = c\,\xi^\omega + O(\xi^{\omega+1})$, $\xi = t - 1$, $\omega \geq 1$. Then the iteration (2.3) satisfies*

$$e_+ = c\,p^{\omega-1} e^{\,\omega+1} + O(e^{\,\omega+2}).$$

*Proof.* From (2.3), $e_+ = e + \log\kappa - \log(\kappa - 1 + t)$, and this vanishes for $\kappa = \kappa_*$. Since $\partial_\kappa[\log\kappa - \log(\kappa - 1 + t)] = (t-1)/[\kappa(\kappa - 1 + t)]$, which equals $\xi/p^2 + O(\xi^2)$ near $\kappa = p$, we get $e_+ = c\,\xi^{\omega+1}/p^2 + O(\xi^{\omega+2})$. Finally $\xi = e^{pe} - 1 = pe + O(e^2)$. □

AK is the value of $\kappa_*$ at $t = 1$, AD its first-order Taylor polynomial and projective AD its [1/1] Padé approximant; these three are classical (Newton under inversion, Halley, and a Padé correction) and are documented in Appendix A. The linear MB construction uses the support $MB$, which does not pass through $A$, and is kept as a baseline in Appendix B.

**Table 3:** The supports as approximations of $\kappa_*$. Leading constants are for the reciprocal-state log error $e$; for odd orders they are unchanged in the direct state.

| Support | $\kappa(t)$ | contact $\omega$ | order | leading constant of $e_+$ |
|---|---|---|---|---|
| AK (Newton) | $p$ | 1 | 2 | $-(p-1)/2$ |
| AD (Halley) | $\frac{1}{2}[p+1+(p-1)t]$ | 2 | 3 | $(p^2-1)/12$ |
| Projective AD | $\dfrac{2p[(2p-1)t+p+1]}{(p+1)t+5p-1}$ | 3 | 4 | $-(p^2-1)(2p-1)/72$ |
| Decentered AD | $1+(p-1)q_5(t)$ | 4 | 5 | $(p-2)(p^2-1)(3p+1)/1440$ |
| Nested radicals | $1+(p-1)q_9(t)$ | 8 | 9 | $c_9(p)$, Theorem 4.1 |
| Three means | $1+(p-1)q_M(t)$ | 8 | 9 | $c_M(p)$, Theorem 5.1 |

### 2.4 Work convention

A *trace* is one join or one compass arc. A constructed parallel expands to $\mathsf{p} = 2\mathsf{j}+3\mathsf{c}$, five traces. Intersections of drawn objects are free. *Fixed preparation*, meaning every object that depends only on $p, X, W, H$ and not on the current state, is not charged, nor are decisions (comparisons of two constructed lengths) or the single final inversion that converts $s$ into $u = 1/s$. Section 7 charges its input and output inversions explicitly. All counts are upper bounds for the specified protocols; a trace count is neither a time nor an energy.

The name Pandrosion refers to the addressee of Book III of Pappus' *Collection* [1]. Our rectangle follows a modern reconstruction [2]; the accelerated supports are modern and are not attributed to the ancient text.

## 3 A decentered arc with global fifth-order convergence

### 3.1 Formula and construction

For real $p > 2$ put

$$S(t) = (p-2)(t^2+1) + (10p+4)t, \qquad q_5(t) = \sqrt{\frac{S(t)}{12p}}, \qquad \mathrm{T}_{\mathrm{arc}}(s) = s\,\frac{1+(p-1)q_5(t)}{t+(p-1)q_5(t)}, \tag{3.1}$$

that is, the support $\kappa = 1+(p-1)q_5(t)$ in (2.3). The radicand is positive for $t > 0$.

For integer $p \geq 3$ the radical is produced by one arc. Put

$$\eta = (p-1)\sqrt{\frac{p-2}{12p}}, \qquad \zeta = \frac{5p+2}{p-2} > 1, \qquad d_0 = \frac{W}{\eta}, \qquad \delta = \frac{H}{X}\sqrt{\zeta^2-1},$$

and prepare

$$G_0 = \Big(W,\ H + \frac{H\zeta}{X}\Big), \qquad O_{\mathrm{arc}} = \Big(W - d_0 + \delta,\ H - \frac{H}{X\eta}\Big), \qquad \text{the vertical } x = W - d_0.$$

Draw the arc centred at $O_{\mathrm{arc}}$ with radius $EG_0 = (H/X)(t+\zeta)$ and take its lower intersection $D_{\mathrm{arc}}$ with the prepared vertical. Its distance below the centre is

$$\sqrt{EG_0^2 - \delta^2} = \frac{H}{X}\sqrt{t^2+2\zeta t+1},$$

so the slope of $AD_{\mathrm{arc}}$ is $\frac{H}{WX}\big[1+\eta\sqrt{t^2+2\zeta t+1}\big] = \frac{H}{WX}\big[1+(p-1)q_5(t)\big]$, because $(p-2)\cdot 2\zeta = 10p+4$. All preparation parameters use rational operations and square roots of positive quantities. Centered AD and decentered AD use the same mobile operations, one arc and one join; only the fixed preparation differs. This is the precise sense in which order five is obtained at the mobile cost of order three.

### 3.2 Global monotone convergence

**Theorem 3.1** (Formalized in Lean)**.** *For real $p > 2$, $X > 0$ and every $s_0 > 0$, the iteration $s_{n+1} = \mathrm{T}_{\mathrm{arc}}(s_n)$ converges to $\alpha$ monotonically without crossing it, and*

$$e_+ = \frac{(p-2)(p^2-1)(3p+1)}{1440}\,e^5 + O(e^7). \tag{3.2}$$

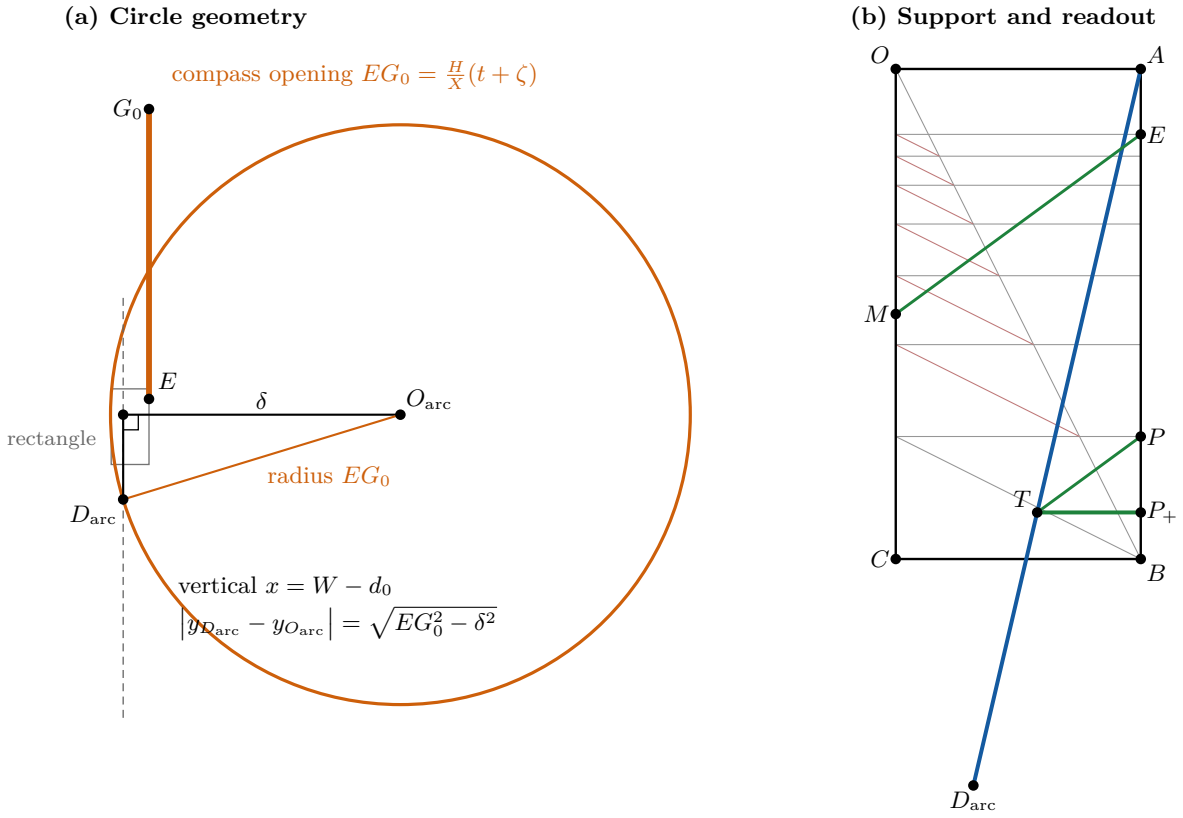



**Figure 1:** The decentered-arc device for $p = 7$, $X = W = 2$, $H = 4$, $s = 3/4$, drawn from the exact coordinates. (a) The whole circle. The compass opening $EG_0$ (thick orange segment) is carried to the prepared centre $O_{\text{arc}}$; the circle meets the prepared vertical at $D_{\text{arc}}$, and the right triangle with horizontal leg $\delta$ shows why its vertical leg is a square root. The small grey box is the rectangle at the same scale. (b) The rectangle enlarged: triangle chain (grey), transport lines (green), support $AD_{\text{arc}}$ (blue) and the readout $P_+$. Each panel has equal axis scales.

*Proof.* Write $g = (p-1)q_5$. Since $S(1/t) = S(t)/t^2$ we have $q_5(1/t) = q_5(t)/t$, hence $\Phi(1/t) = 1/\Phi(t)$ for $\Phi = (1+g)/(t+g)$: the log-error map $e \mapsto e_+$ is odd. Put

$$\Lambda(t) = \frac{\log t}{p} + \log(1+g(t)) - \log(t+g(t)),$$

so that $e_+ = \Lambda(t)$, and define the polynomials

$$\begin{aligned} N_1(t) &= (p-1)(t^2+1) + (10p+2)t, \\ N_2(t) &= (t+1)\big(6pt - (t-1)^2\big), \\ N_3(t) &= (p^2-5p-2)(t-1)^2 + 12p(3p+1)t. \end{aligned}$$

Differentiation and factorization give the two identities

$$\frac{d\Lambda}{d\log t} = \frac{(p-2)(p-1)^2\left(q_5 N_1 - N_2\right)}{12p^2\, g(1+g)(t+g)}, \tag{3.3}$$

$$q_5^2 N_1^2 - N_2^2 = \frac{p+1}{12p}\,(t-1)^4\, N_3. \tag{3.4}$$

Here $N_1 > 0$. If $N_2 \le 0$ then $q_5 N_1 - N_2 > 0$. Otherwise $(t-1)^2 < 6pt$, and $N_3 > 0$: directly when $p^2 - 5p - 2 \ge 0$, and otherwise from the rearrangement

$$N_3 = 6p^2(p+1)t + (p^2-5p-2)\big((t-1)^2 - 6pt\big),$$

whose two terms are positive. Then (3.4) gives $q_5 N_1 > N_2$ for $t \ne 1$. Hence $\Lambda$ is strictly increasing with $\Lambda(1) = 0$: the new log error has the sign of the old one. Meanwhile $\Phi(t) - 1 = (1-t)/(t+g)$ moves the state toward $\alpha$. The orbit is monotone and bounded between $s_0$ and $\alpha$; its positive limit is a fixed point by continuity, and $\Phi(t) = 1$ forces $t = 1$.

Near $t = 1$, rationalize $q_5N_1 - N_2$ with (3.4). At $t = 1$ one has $q_5 = 1$, $g = p - 1$, $N_1 = N_2 = 12p$ and $N_3 = 12p(3p + 1)$, so

$$\lim_{t\to 1} \frac{d\Lambda/d\log t}{(t-1)^4} = \frac{(p-2)(p^2-1)(3p+1)}{288\,p^5}.$$

Substituting $t = e^{pe}$ and integrating yields the coefficient in (3.2); oddness removes the $e^6$ term. □

At $p = 3$ the constant is $1/18$. At $p = 2$ the scalar formula is an exact square-root correction, but the displayed preparation is singular and is replaced by a single mean proportional.

# 4 A nested-radical support of order nine

The next support uses two successive mean proportionals, the output of the first entering the diameter of the second. In this section it is convenient to follow the direct state $u = 1/s$ with target $r = X^{1/p}$ and log error $\hat{e} = \log(u/r) = -e$. The residual is unchanged, $t = X/u^p = Xs^p$, so the rail encoding of Section 2 is unchanged.

## 4.1 Formula, domain and rectangle support

For $p > 2$ write $h = 1/p$ and define

$$a_9 = \frac{1-2h}{12}, \qquad b_9 = \frac{(h+1)(h+3)}{30}, \qquad c_9 = \frac{121 - 185h - 67h^2 - h^3}{840(h+3)}, \tag{4.1}$$

$$w = \frac{(t-1)^2}{t}, \qquad k_9 = \sqrt{1 + \frac{b_9 w}{1 + c_9 w}}, \qquad q_9 = \sqrt{t\Big(1 + \frac{a_9 w}{k_9}\Big)}. \tag{4.2}$$

All square roots are positive branches. The iteration is

$$\Gamma_p(t) = \frac{t + (p-1)q_9(t)}{1 + (p-1)q_9(t)}, \qquad F_{p,X}(u) = u\,\Gamma_p\big(X/u^p\big), \tag{4.3}$$

which is the support $\kappa = 1 + (p-1)q_9$ in (2.3), read in the direct state.

For $0 < h < 1/2$ the three coefficients are positive: the numerator of $c_9$ is decreasing on this interval and equals $93/8$ at $h = 1/2$. Thus every division and radical in (4.2) is defined for every $t > 0$. Moreover

$$w(1/t) = w(t), \qquad q_9(1/t) = q_9(t)/t, \qquad \Gamma_p(1/t) = 1/\Gamma_p(t), \tag{4.4}$$

so the log-error map $\hat{e} \mapsto \hat{e}_+$ is odd.

In the rectangle, one support point is $D_9 = \big(0,\ H - \frac{H}{X}(1 + (p-1)q_9)\big)$. The parallel to $ME$ through $P = R(s)$ meets $AD_9$, and the horizontal readout gives $s_+ = s\,(1 + (p-1)q_9)/(t + (p-1)q_9)$, i.e. $1/s_+ = F_{p,X}(u)$. After $t$ is obtained, the arithmetic consists of rational operations and two mean proportionals, $k_9 = \sqrt{1 \cdot (1 + b_9 w/(1 + c_9 w))}$ and $q_9 = \sqrt{t \cdot (1 + a_9 w/k_9)}$.

## 4.2 First complete step for the cube root of two

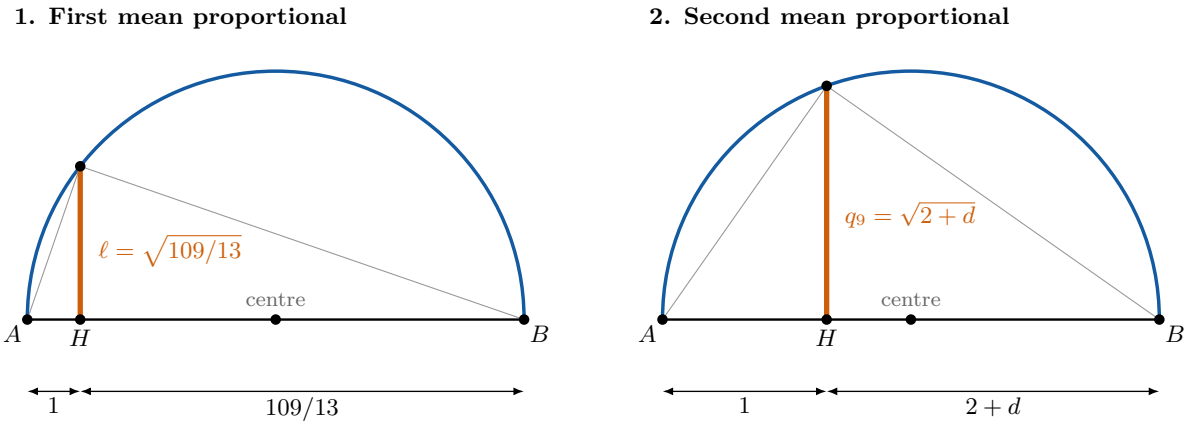
At $p = 3$ the support simplifies to

$$q_9(t) = \sqrt{t + \frac{(t-1)^2}{108}\sqrt{\frac{t^2 + 52t + 1}{t^2 + 4t + 1}}}, \qquad u_+ = u\,\frac{t + 2q_9(t)}{1 + 2q_9(t)}. \tag{4.5}$$

Here is the first step for $X = 2$, $u_0 = 1$. The auxiliary diagrams have their own local point names. The unknown cube root is never used to place a point.

1. *Rational preparation.* The residual is $t = 2$. Prepare $109/13$ and $1/108$ by subdivisions and similar triangles.

2. *First semicircle.* Place adjacent segments of lengths 1 and $109/13$, draw the semicircle on their sum and the perpendicular at the junction. Its height is $\ell = \sqrt{109/13} = 2.895620034572\ldots$ (This cubic auxiliary is not the general $k_9$.)
3. *Second diameter.* A similar-triangle division gives $d = \ell/108 = 0.026811296616\ldots$; add it to two units.
4. *Second semicircle.* With adjacent lengths 1 and $2 + d$ the perpendicular height is $q_9 = \sqrt{2 + d} = 1.423661229583\ldots$
5. *Move the support.* Choose $W = 6$, $H = 4$, so $M = (0, 2)$. Here $s_0 = 1$, hence $P_0 = E = B$. Place $D_9 = (0,\, 2 - 4q_9)$ below $M$.
6. *Intersect and report.* Draw $AD_9$ and $MB$; they meet at $T_9$. The horizontal through $T_9$ meets $AB$ at $P_1$, and the rectangle reports $s_1 = AP_1/AB$.
7. *Invert.* A similar-triangle construction produces $u_1 = AB/AP_1$.




Between the two: prepare $d = \ell/108$ by similar triangles, then transfer $2 + d$ to the second diameter.

**Figure 2:** The two successive mean proportionals for $X = 2$, $u_0 = 1$. Each panel has equal axis scales and its own magnification. The orange perpendiculars are the constructed lengths; the first height supplies the rationally scaled addition $d$ used by the second diameter.

The incidences give

$$\begin{aligned} T_9 &= (3.524406494288\ldots,\ 0.825197835237\ldots), \\ s_1 &= 0.79370054119068191329\ldots, \\ u_1 &= 1.25992102575592908435636220628 1\ldots, \end{aligned}$$

with relative error $u_1/r - 1 \approx -1.9159092613 \times 10^{-8}$. These digits describe exact geometric incidences evaluated numerically; they are not readable to that precision from a manual drawing. Later steps recompute $t = 2/u^3$: the constants 109 and 13 belong to this first step only. The seven grouped instructions above, like the twelve screens of the companion interactive display, are pedagogical steps and not primitive trace counts; those are in Section 6.

## 4.3 Local order: exactly nine for every real $p > 2$

The exact support corresponds to $q_* = (\kappa_* - 1)/(p - 1) = (t - t^h)/[(p - 1)(t^h - 1)]$, used only in the analysis. With $x = \log t$ and quotients interpreted continuously at zero,

$$Y := \frac{q_*^2}{t} = \left[\frac{\sinh((1-h)x/2)\,/\,((1-h)x/2)}{\sinh(hx/2)\,/\,(hx/2)}\right]^2, \qquad w = 2(\cosh x - 1).$$

Both sides are even in $x$, so $Y$ is a power series in $w$:

$$\begin{aligned} Y &= 1 + a_9 w + A_2 w^2 + A_3 w^3 + O(w^4), \\ A_2 &= -\frac{(1-2h)(h+1)(h+3)}{720}, \qquad A_3 = \frac{(1-2h)(h+1)(2h^3+8h^2+13h+31)}{60480}, \end{aligned} \tag{4.6}$$

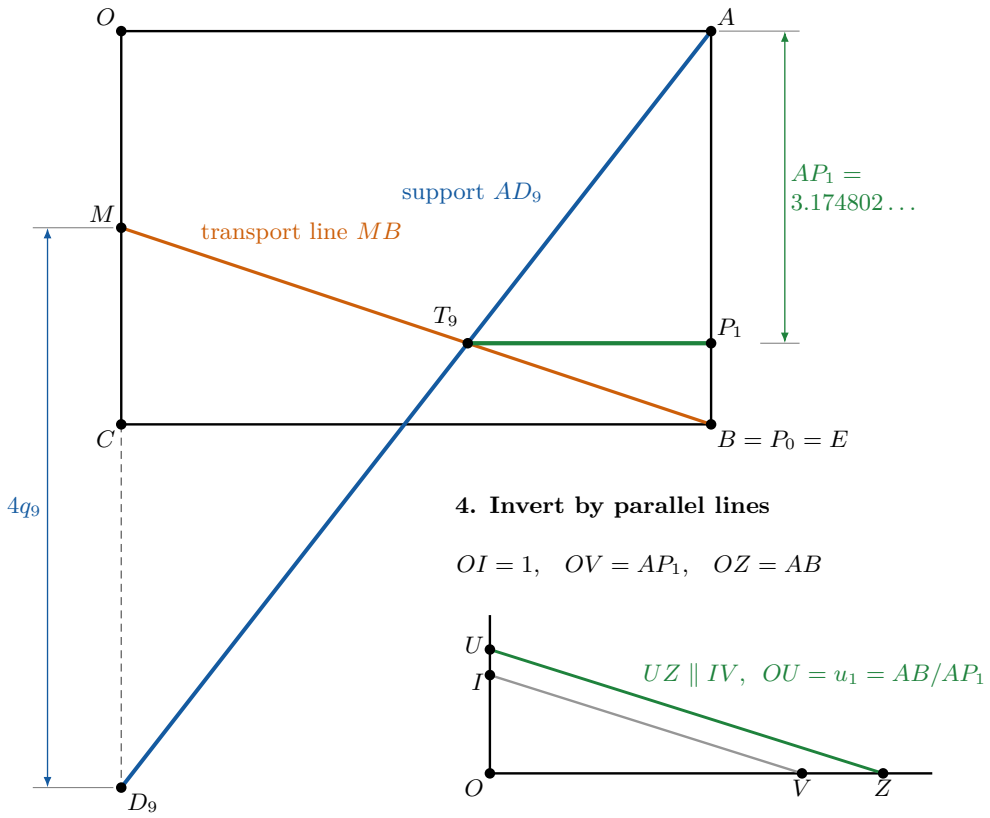



**Figure 3:** The modified Pandrosion support for the same first step, at equal axis scales. The support $AD_9$ (blue) meets the transport line (orange) at $T_9$, and the horizontal (green) reads $P_1$. Because $s_0 = 1$, $P_0 = E = B$ and the transport line is $MB$ itself. The extension below $C$ is part of the construction. Lower right: the reciprocal reading $u_1 = AB/AP_1$ by parallel lines.

while the proposed support has

$$\frac{q_9^2}{t} = 1 + a_9 w - \frac{a_9 b_9}{2}\, w^2 + a_9\Big(\frac{b_9 c_9}{2} + \frac{3b_9^2}{8}\Big) w^3 + O(w^4). \tag{4.7}$$

The coefficients (4.1) are exactly those that make (4.7) agree with (4.6) through $w^3$. The first unmatched term is explicit.

**Theorem 4.1** (Order nine with explicit constant; formalized in Lean)**.** *For every real $p > 2$ and $X > 0$, the iteration $u_+ = F_{p,X}(u)$ satisfies*

$$\hat{e}_+ = c_9(p)\, \hat{e}^{\,9} + O(\hat{e}^{\,11}), \qquad c_9(p) = \frac{(p^2-1)(p-2)\, N_9(p)}{2^{11}\, 3^4\, 5^3\, 7^2\, (3p+1)}, \tag{4.8}$$

$$N_9(p) = 21311p^6 + 1650p^5 - 21679p^4 - 15532p^3 - 4411p^2 - 526p - 29.$$

*Moreover $c_9(p) > 0$ for every $p > 2$, so the local order is exactly nine. In particular $c_9(3) = 7/648$.*

*Proof.* Continuing the two expansions one term further gives

$$\frac{q_9^2}{t} - Y = D_4\, w^4 + O(w^5), \qquad D_4 = \frac{(1-2h)(1+h)\, n_9(h)}{2^{10}\, 3^4\, 5^3\, 7^2\, (h+3)}, \tag{4.9}$$

with $n_9(h) = 21311 + 1650h - 21679h^2 - 15532h^3 - 4411h^4 - 526h^5 - 29h^6 = h^6 N_9(1/h)$. This is an identity between rational functions of $h$, obtained by exact series expansion. (In the Lean proof it is obtained without Taylor series: $h^2t^4(t-t^h)^2 - (1-h)^2 t(t^h-1)^2\, t^4 P_4(w)$, with $P_4$ the quartic part of (4.6), is a sum of 27 exponentials $c_j e^{\lambda_j x}$ whose moments $\sum_j c_j \lambda_j^n$ vanish for $n < 12$, hence it is $O(x^{12})$.) Since $w = \xi^2/t$ and

$q_9 + q_* \to 2$ as $t \to 1$, we get $q_9 - q_* = \frac{1}{2}D_4\xi^8 + O(\xi^9)$ and therefore $\kappa - \kappa_* = \frac{1}{2}(p-1)D_4\,\xi^8 + O(\xi^9)$. Lemma 2.1 with $\omega = 8$ gives $e_+ = \frac{1}{2}(p-1)p^7 D_4\, e^9 + O(e^{10})$. Substituting $h = 1/p$,

$$\tfrac{1}{2}(p-1)p^7 D_4 = \frac{(p-1)(p-2)(p+1)N_9(p)}{2^{11}3^4 5^3 7^2(3p+1)} = c_9(p).$$

By (4.4) the map is odd, so the same expansion holds for $\hat{e} = -e$ and the next term is of order eleven. For positivity,

$$N_9(2+\rho) = 21311\rho^6 + 257382\rho^5 + 1273481\rho^4 + 3286796\rho^3 + 4628741\rho^2 + 3325430\rho + 926859,$$

which has only positive coefficients; hence $N_9(p) > 0$ and $c_9(p) > 0$ for $p > 2$. Finally $N_9(3) = 13720000$ gives $c_9(3) = 8 \cdot 13720000/(1016064000 \cdot 10) = 7/648$. □

*Remark* 4.2 (Scale of the constant). $c_9(p)$ grows like $p^8$: for instance $c_9(4) \approx 0.187$, $c_9(7) \approx 26.6$ and $c_9(20) \approx 1.58 \times 10^5$. This is the natural scale, not a deterioration. In the residual logarithm $x = \log t = -p\hat{e}$ the law reads $x_+ = c_9(p)p^{-8}x^9 + \dots$, and $c_9(p)p^{-8} \to 21311/3048192000 \approx 7.0 \times 10^{-6}$ as $p \to \infty$. The same rescaling applied to (3.2) gives the limit $1/480$ for the decentered arc. The asymptotic regime is $|x| \lesssim 1$, that is $|\hat{e}| \lesssim 1/p$, for both.

For the cubic specialization a short positive certificate proves the constant independently of series manipulations; it was the first version formalized in Lean. Let $v = t^{1/3} > 0$ and set

$$\begin{aligned} D_v &= v^6 + 4v^3 + 1, \\ H_v &= v^8 + 10v^7 + 55v^6 + 268v^5 + 466v^4 + 268v^3 + 55v^2 + 10v + 1, \\ \Theta_v &= (v^2+v+1)^2\sqrt{(v^6+52v^3+1)/D_v}. \end{aligned}$$

The exact identity

$$(v^2+v+1)^4(v^6+52v^3+1) - 729v^4 D_v = (v-1)^6 H_v \tag{4.10}$$

implies $\Theta_v \geq 27v^2$ and gives

$$q_9^2 - \Big(\frac{v^2+v}{2}\Big)^2 = \frac{(v-1)^8 H_v}{108\, D_v\,(\Theta_v + 27v^2)}, \tag{4.11}$$

where every denominator is positive. Since $H_1 = 1134$, $q_9 - \frac{1}{2}(v^2+v) = \frac{7}{432}(v-1)^8 + O((v-1)^9)$.

**Theorem 4.3** (Cubic certificate; formalized in Lean). *For $X > 0$ and $r = X^{1/3}$,*

$$\lim_{u \to r,\ u \neq r} \frac{F_{3,X}(u)/r - 1}{(u/r-1)^9} = \frac{7}{648}.$$

*Proof.* With $y = u/r$ one has $v = 1/y$. The exact difference $\Gamma_3(v^3) - v$ equals $2(1-v)\big(q_9 - \frac{1}{2}(v^2+v)\big)/(1+2q_9)$. Substituting (4.11) and $v = 1/y$ factors $F_{3,1}(y) - 1$ as $(y-1)^9$ times a continuous positive function with value $7/648$ at one. The scaling $F_{3,r^3}(ry) = rF_{3,1}(y)$ gives the limit. □

## 4.4 Global convergence for every real degree greater than two

Local cancellation says nothing about distant starts. An independent sign argument covers the whole positive axis.

**Theorem 4.4** (Global monotone convergence; formalized in Lean). *For every real $p > 2$, $X > 0$ and $u_0 > 0$, the iteration $u_{n+1} = F_{p,X}(u_n)$ is defined, stays positive and converges to $r = X^{1/p}$. If $u_0 \neq r$ it moves strictly toward $r$ without crossing it.*

*Proof.* We give the reduction to positive polynomial certificates; the complete integer coefficients are in the Lean source, and their structure was recomputed independently for this revision (Section 9). Define

$$\mathcal{E} = 840p^2(3p+1), \qquad \mathcal{C} = 121p^3 - 185p^2 - 67p - 1, \qquad \mathcal{D} = 373p^3 + 235p^2 + 129p + 27,$$
$$\mathcal{U} = \mathcal{E} + \mathcal{C}w, \qquad \mathcal{V} = \mathcal{E} + \mathcal{D}w, \qquad \mathcal{L} = \sqrt{\mathcal{U}/\mathcal{V}}, \qquad \mathcal{R} = 1 + \frac{(p-2)w\mathcal{L}}{12p}.$$

Then $\mathcal{L} = 1/k_9$ and $q_9 = \sqrt{t\mathcal{R}}$. For $p > 2$ and $w \geq 0$ the quantities $\mathcal{U}, \mathcal{V}, \mathcal{L}, \mathcal{R}$ are positive. Put

$$\mathcal{J} = 4\mathcal{U}\mathcal{V} - p\,\mathcal{E}(\mathcal{D} - \mathcal{C})w, \qquad \mathcal{A} = 1 + \frac{(p-1)w\mathcal{L}}{12p}, \qquad \mathcal{B} = 1 - \frac{\mathcal{J}w\mathcal{L}}{24p\mathcal{U}\mathcal{V}}.$$

A two-region certificate establishes

$$0 < w \leq 30p \implies \mathcal{R}\mathcal{A}^2 > (1 + w/4)\,\mathcal{B}^2, \tag{4.12}$$

$$w \geq 30p \implies \mathcal{B} < 0. \tag{4.13}$$

The elimination uses

$$\mathcal{K} = -1728p^3\mathcal{U}\mathcal{V}^3 + 48p(p-1)(3p-5)\,\mathcal{U}^2\mathcal{V}^2w - 3p\,\mathcal{J}^2(4+w)w,$$
$$\mathcal{M} = 576p^2(3p-4)\,\mathcal{U}\mathcal{V} + 144p^2\mathcal{J}(4+w) + 4(p-2)(p-1)^2\,\mathcal{U}^2w^2.$$

There is a polynomial $\mathcal{P}(p, w)$, of degree nine in $w$ and twenty-nine in $p$, with

$$(\mathcal{V}^2\mathcal{M})^2\,\mathcal{U} - \mathcal{K}^2\,\mathcal{V} = (p+1)\,w^3\,\mathcal{V}\,\mathcal{P}(p, w),$$

and it has the exact Bernstein form

$$(30p)^9\,\mathcal{P}(p, w) = \sum_{j=0}^{9} w^j(30p - w)^{9-j}\,T_j(p-2), \tag{4.14}$$

in which every $T_j$ is a polynomial with only positive coefficients, 345 terms in all. Hence $\mathcal{P} > 0$ for $p > 2$, $0 \leq w \leq 30p$. Positive-coefficient expansions of $\mathcal{M}$ in $(p-2, w)$, and of $\mathcal{J}$ and $w^2\mathcal{J}^2 - 576p^2\mathcal{U}\mathcal{V}^3$ in $(p-2,\ w-30p)$, with 49, 24 and 112 terms respectively, provide the remaining signs. Rationalizing with $\mathcal{L}^2\mathcal{V} = \mathcal{U}$ proves (4.12) and (4.13). These are exact identities and inequalities, not sampled signs.

Since $(t+1)^2 = 4t(1 + w/4)$ and $q_9^2 = t\mathcal{R}$, the two regions give

$$2q_9\mathcal{A} - (t+1)\mathcal{B} > 0 \qquad (t > 0,\ t \neq 1). \tag{4.15}$$

Define $\Delta_p(t) = \log\Gamma_p(t) - \log(t)/p$. Exact differentiation yields

$$\Delta_p'(t) = -\frac{(p-1)(p-2)\left[2q_9\mathcal{A} - (t+1)\mathcal{B}\right]}{2p\,q_9\,[t + (p-1)q_9]\,[1 + (p-1)q_9]} < 0 \qquad (t \neq 1). \tag{4.16}$$

With $\Delta_p(1) = 0$ and $\Gamma_p(t) - 1 = (t-1)/(1 + (p-1)q_9)$ this proves

$$t > 1:\ 1 < \Gamma_p(t) < t^{1/p}, \qquad 0 < t < 1:\ t^{1/p} < \Gamma_p(t) < 1.$$

Consequently $u < F_{p,X}(u) < r$ below the root and $r < F_{p,X}(u) < u$ above it. The orbit is monotone and bounded, its limit is positive, continuity makes it a fixed point, and $\Gamma_p(t) = 1$ forces $t = 1$. □

## 4.5 Which degrees give a finite construction

Theorems 3.1, 4.1 and 4.4, and Theorem 5.1 of the next section, are statements about real functions of a real parameter $p$. A drawing needs more: the residual $t = X/u^p$ must be *constructed* at every step. The triangle stage constructs integer powers only. This subsection says exactly what follows.

**Proposition 4.5** (Rational degrees are finite constructions)**.** *Let $p = \mu/\nu$ with coprime positive integers $\mu, \nu$, and $X > 0$. Then $X^{1/p} = (X^\nu)^{1/\mu}$, and:*

*(i) if $\mu \geq 3$, every integer-degree protocol of this paper applies with degree $\mu$ and input $X^\nu$. In particular the decentered, nested and three-mean iterations converge monotonically from every positive start, with orders five, nine and nine, at no more than $10\mu + 9$, $10\mu + 59$ and $10\mu + 11$ traces per step (Section 6). The input $X^\nu$ is fixed preparation: $\nu - 1$ five-join products, once;*

*(ii) if $\mu \in \{1, 2\}$, the root $X^\nu$ or $\sqrt{X^\nu}$ is constructed exactly, by $\nu - 1$ products and at most one mean proportional.*

*For $p < 0$ apply the above to $|p|$ and invert the output (five joins, once).*

*Proof.* The residual of the degree-$\mu$ problem with input $X^\nu$ is $t = X^\nu s^\mu$, built by the triangle stage with $\mu$ in place of $p$ from the prepared point $M = (0, H(1 - X^{-\nu}))$. Theorems 3.1, 4.4 and 5.1 apply with real degree $\mu > 2$ and positive input $X^\nu$, and their fixed point is $(X^\nu)^{1/\mu}$. □

Two consequences are worth stating. First, the degree seen by the iteration is $\mu$, not $p$: the degree $p = 3/2$ is handled as a cube root of $X^2$, inside the domain $\mu > 2$ of the unmodified formulas although $3/2 < 2$. Second, the cost is governed by $\mu$: $p = 355/113$ costs as much per step as degree 355.

The restriction to degree greater than two is real for the *raw* formula. For $p = 3/2$, $t = 100$ one has $c_9 = -25/2376$, $1 + c_9 w = -1/32$ and $1 + b_9 w/(1 + c_9 w) = -15947/25 < 0$, so $k_9$ is not real; Lean checks this counterexample. As a scalar statement the restriction can be removed:

**Proposition 4.6** (Scalar extension to every nonzero real degree; formalized in Lean)**.** *For every real $p \neq 0$, every $X > 0$ and every start $u_0 > 0$ there is an explicit modification of (4.3) that converges monotonically to $X^{1/p}$ without crossing it.*

*Proof.* Choose an integer $k \geq 0$ with $p' = 2^k|p| > 2$. For $p > 0$ put $v_0 = u_0^{1/2^k}$, iterate $v_{n+1} = F_{p',X}(v_n)$ and report $u_n = v_n^{2^k}$; for $p < 0$ put $v_0 = u_0^{-1/2^k}$ and report $u_n = v_n^{-2^k}$. The reported start is exactly $u_0$. Theorem 4.4 gives $v_n \to X^{1/p'}$, so $u_n \to X^{\pm 2^k/p'} = X^{1/p}$. Positive integer powers preserve inequalities and inversion reverses them together with the direction of approach. For $p > 2$ take $k = 0$. □

Proposition 4.6 is a change of variable and adds no geometric content beyond Proposition 4.5: for irrational $p$ the step still needs the real power $v^{p'}$, which is a problem of the same nature as the root being sought. Irrational degrees can nevertheless be reached by the fast iterations through a rational approximation of $p$, with a controlled error:

**Proposition 4.7** (Irrational degrees by rational approximation)**.** *Let $p > 0$ be real, $X > 0$, $r = X^{1/p}$, and let $\mu, \nu$ be positive integers with $\left|\nu/\mu - 1/p\right| \leq \eta$. Then $r' = X^{\nu/\mu}$ satisfies*

$$\left|\frac{r'}{r} - 1\right| \leq e^{\eta|\log X|} - 1.$$

*If moreover $\tilde{u} > 0$ satisfies $|\tilde{u}/r' - 1| \leq \varepsilon_1$, then $|\tilde{u}/r - 1| \leq (1 + \varepsilon_1)\, e^{\eta|\log X|} - 1$.*

*Proof.* $r'/r = X^{\nu/\mu - 1/p}$, so $|\log(r'/r)| \leq \eta|\log X|$, which gives the first bound since $1 - e^{-y} \leq e^y - 1$ for $y \geq 0$. For the second, $\tilde{u}/r = (\tilde{u}/r')(r'/r)$ lies between $(1 - \varepsilon_1)e^{-y}$ and $(1 + \varepsilon_1)e^y$ with $y = \eta|\log X|$, and $1 - (1 - \varepsilon_1)e^{-y} \leq (1 + \varepsilon_1)e^y - 1$. □

*Remark* 4.8 (Cost of the rational route). Take $p = \pi$, $X = 2$, $r = 2^{1/\pi} = 1.2468689889\ldots$ With $\mu/\nu = 22/7$, $\eta \approx 1.28 \times 10^{-4}$ and the approximation error is at most $8.9 \times 10^{-5}$; a step costs at most 229 traces (decentered), 231 (three means) or 279 (nested), after 30 joins of preparation. With $\mu/\nu = 355/113$, $\eta \approx 2.70 \times 10^{-8}$ and the error is at most $1.9 \times 10^{-8}$, but a step costs at most 3559, 3561 or 3609 traces after 560 joins of preparation. The direct subdivision of Section 7 reaches relative width $10^{-8}$ for the true exponent in at most 123 traces. Since a convergent $\nu/\mu$ of $1/p$ has $\eta$ of order $\mu^{-2}$, the rational route needs $\mu$ of order $\varepsilon^{-1/2}$ for accuracy $\varepsilon$, while its step cost is linear in $\mu$. For irrational degrees the subdivision is therefore the recommended calculator, and the rational route is of interest only when a small $\mu$ is acceptable.

A third route would approximate the real power $u^p$ inside each step by an inner subdivision. That is a two-level recursion whose outer iteration receives an inexact residual; its convergence would need a perturbation analysis that we have not carried out (Section 11).

## 4.6 Algebraic character of the correction

At $p = 3$, $t = 2$,

$$q_9^2 = 2 + \frac{\sqrt{109/13}}{108}, \qquad N_{\mathbb{Q}(\sqrt{109/13})/\mathbb{Q}}\left(q_9^2\right) = \frac{606419}{151632}.$$

Neither this norm nor $109/13$ is a rational square, so $q_9$ has degree four over $\mathbb{Q}$. The correction $(2 + 2q_9)/(1 + 2q_9)$ is an invertible homography of $q_9$ and also has degree four. Hence the cubic correction is not a rational function of $t$ with rational coefficients, and cannot be written in this normalization with a single square root over $\mathbb{Q}$. This is an exact rational computation, not one of the Lean theorems.

The argument does not exclude generalized algebraic or Hermite–Padé approximants, transformed targets or other changes of variable. Algebraic approximants of arbitrary degree are established generalizations of Padé approximation [3], and the coefficient matching of (4.6)–(4.7) belongs to that methodology. Appendix C discusses what "the same formula up to conjugacy" can and cannot mean for the decentered arc.

# 5 A three-mean support of order nine

The nested support reaches order nine with two radicals placed one inside the other, and its arguments cost divisions. A second support of the same order uses two radicals placed side by side, each of them produced by one arc. It is a combination of three classical means of 1 and $t$.

## 5.1 Formula

The exact support is $\kappa_* = 1 + (p-1)q_*$ with

$$q_*(t) = \frac{t - t^h}{(p-1)(t^h - 1)}, \qquad q_*(1) = 1, \qquad q_*(1/t) = q_*(t)/t,$$

a homogeneous symmetric mean of 1 and $t$; for integer $p$ it is the arithmetic mean of the $p-1$ mean proportionals $t^{k/p}$ between 1 and $t$. For real $p > 2$ define

$$\begin{aligned} m &= \frac{(p-2)(47p^2+21p+4)}{60\,p\,(4p^2-1)}, \qquad & g &= \frac{16\,(p+1)(4p^2-1)}{15\,p\,(5p^2+4)}, \\ n &= \frac{49\,p\,(p+1)(p^2-4)}{10\,(4p^2-1)(5p^2+4)}, \qquad & d &= \frac{5p^2+4}{84\,p^2}, \end{aligned} \tag{5.1}$$

all positive, with $2m + g - n = 1$, and

$$q_M(t) = m\,(1+t) + g\sqrt{t} - n\sqrt{t + d\,(t-1)^2}, \qquad \mathrm{T}_M(s) = s\,\frac{1 + (p-1)q_M(t)}{t + (p-1)q_M(t)}, \tag{5.2}$$

that is, the support $\kappa = 1 + (p-1)q_M(t)$ in (2.3). With the arithmetic mean $\mathrm{A} = (1+t)/2$, the geometric mean $\mathrm{G} = \sqrt{t}$ and the *conic mean* $\mathrm{C}_d = \sqrt{\mathrm{G}^2 + 4d(\mathrm{A}^2 - \mathrm{G}^2)}$,

$$q_M = 2m\,\mathrm{A} + g\,\mathrm{G} - n\,\mathrm{C}_d,$$

a combination with weights of sum one; one weight is negative. The radicand $t + d(t-1)^2$ is positive for every $t > 0$, so $q_M$ is defined on the whole positive axis, and $q_M(1/t) = q_M(t)/t$: the log-error map is odd. In terms of $h = 1/p$, $m = \frac{(1-2h)(4h^2+21h+47)}{60(4-h^2)}$, $g = \frac{16(1+h)(4-h^2)}{15(4h^2+5)}$, $n = \frac{49(1+h)(1-4h^2)}{10(4-h^2)(4h^2+5)}$ and $d = \frac{4h^2+5}{84}$. For cube roots

$$q_M(t) = \frac{7}{90}(1+t) + \frac{64}{63}\sqrt{t} - \frac{6}{35}\sqrt{t + \frac{7}{108}(t-1)^2}. \tag{5.3}$$

The three terms belong to one family. The decentered arc is $q_5^2 = t + a_9(t-1)^2$, with the $a_9$ of (4.1); the members $a = \frac{1}{4}$ and $a = 0$ of the family $q^2 = t + a(t-1)^2$ are A and G, and $\mathrm{C}_d$ is the member $a = d$. Each member divided by $\sqrt{t}$ is $\sqrt{1 + aw}$, a function of $w = (t-1)^2/t$ alone, as is $q_*/\sqrt{t}$. A combination of members therefore matches $q_*/\sqrt{t}$ coefficient by coefficient in $w$: the arc, with one free parameter, matches one coefficient, and (5.2), with three free parameters (four coefficients, one normalization), matches three. The two members A and G are imposed; only the third is chosen by the matching.

## 5.2 Construction by three arcs

Let $\lambda = H/X$, so that $M = (0, H - \lambda)$ and $E = (W, H - \lambda t)$. Put

$$\gamma = 1 + 2(p-1)m, \qquad \zeta = \frac{1}{2d} - 1 > 1, \qquad K_g = \frac{(p-1)g}{\gamma}\,\lambda, \qquad K_n = \frac{(p-1)n\sqrt{d}}{\gamma}\,\lambda,$$

and prepare four verticals, the horizontal through $M$ and three points:

$$v:\ x = W\Big(1-\frac{1}{\gamma}\Big), \qquad v_1:\ x = x_1 = \frac{(p-1)m}{\gamma}W, \qquad v_2:\ x = x_2 = \frac{K_g}{2\lambda}W, \qquad v_3:\ x = x_3 = \frac{K_n}{\lambda}W,$$
$$F = (x_2,\, H-\lambda), \qquad G_2 = (x_2,\, H-\lambda+K_g), \qquad G_3 = (x_3,\, H-\lambda+K_n(1+\zeta)).$$

The vertical $v$ is at abscissa $2x_1$. The construction below requires that the distance from $v_1$ to $v$ equal $K_n\sqrt{\zeta^2-1}$, which fixes the shape of the rectangle:

$$\frac{WX}{H} = \frac{n}{m}\sqrt{\frac{1-4d}{4d}}. \tag{5.4}$$

The right side is a constructible number depending on $p$ only; it equals $3.7256\ldots$ for $p=3$ and decreases to $2.238\ldots$ as $p\to\infty$.

The line $ME$ is drawn for the transport. Its intersections $J_i = ME\cap v_i$ are free, and their heights are affine in $t$: $y_{J_i} = H-\lambda+(x_i/W)\lambda(1-t)$. Three arcs follow.

1. *Conic radical.* With centre $J_1$ and compass opening $J_3G_3 = K_n(t+\zeta)$, draw an arc and take its upper intersection $D_1$ with $v$. Its height above $J_1$ is $K_n\sqrt{(t+\zeta)^2-(\zeta^2-1)} = K_n\sqrt{(t+d(t-1)^2)/d}$. This is the device of the decentered arc, with a moving centre.
2. *Mean proportional.* With centre $J_2$, draw the arc through $G_2$; its radius is $\frac{1}{2}K_g(1+t)$ and $J_2$ is at distance $\frac{1}{2}K_g|1-t|$ from the horizontal through $M$, so the arc meets that horizontal at a point $Z$ with $FZ = K_g\sqrt{t}$.
3. *Transfer.* With centre $D_1$ and opening $FZ$, draw an arc and take its lower intersection $D_M$ with $v$.

Then

$$H - y_{D_M} = \frac{\lambda}{\gamma}\big[1+(p-1)m(1+t)\big] - K_n\sqrt{\frac{t+d(t-1)^2}{d}} + K_g\sqrt{t} = \frac{\lambda}{\gamma}\big[1+(p-1)q_M(t)\big],$$

and since $W - x_{D_M} = W/\gamma$ the slope of $AD_M$ is $\frac{H}{WX}[1+(p-1)q_M(t)]$: the join $AD_M$ is the support. Both radicands are positive for $t>0$, so the three intersections exist at every state. The mobile work is three arcs and one join, against one arc and one join for the decentered arc. Without the condition (5.4) the centre of the first arc is obtained by one additional join, projecting $E$ from a prepared point onto the vertical at distance $K_n\sqrt{\zeta^2-1}$ from $v$; we count the protocol with (5.4).

## 5.3 Global convergence and order nine

**Theorem 5.1** (Three-mean support; formalized in Lean)**.** *For real $p>2$, $X>0$ and every $s_0>0$:*

(i) $q_M(t)>0$ *for every* $t>0$*;*

(ii) *the iteration* $s_{j+1} = \mathrm{T}_M(s_j)$ *converges to* $\alpha$ *monotonically without crossing it;*

(iii) *the local order is exactly nine,*

$$e_+ = c_M(p)\,e^9 + O(e^{11}), \qquad c_M(p) = \frac{(p^2-1)(p^2-4)(4p^2-1)(17p^2+8)}{2^{11}\,3^4\,5^2\,7^2} > 0, \tag{5.5}$$

*and* $c_M(3) = 23/20736$.

For comparison $c_9(3) = 7/648 = 224/20736$: at $p=3$ the constant is about ten times smaller than that of the nested support, and $c_M(p)/c_9(p)\to 1020/21311\approx 0.048$ as $p\to\infty$.

*Proof.* Work in the variable $\tau = \sqrt{t}>0$, in which only one radical remains. Put $c = p-1$ and

$$S_M(\tau) = \tau^2 + d\,(\tau^2-1)^2, \qquad \rho_M = \sqrt{S_M}, \qquad \ell_M(\tau) = m(1+\tau^2) + g\,\tau, \qquad q(\tau) = \ell_M(\tau) - n\,\rho_M(\tau),$$

so that $q_M(t) = q(\sqrt{t})$ and $S_M\ge\tau^2>0$.

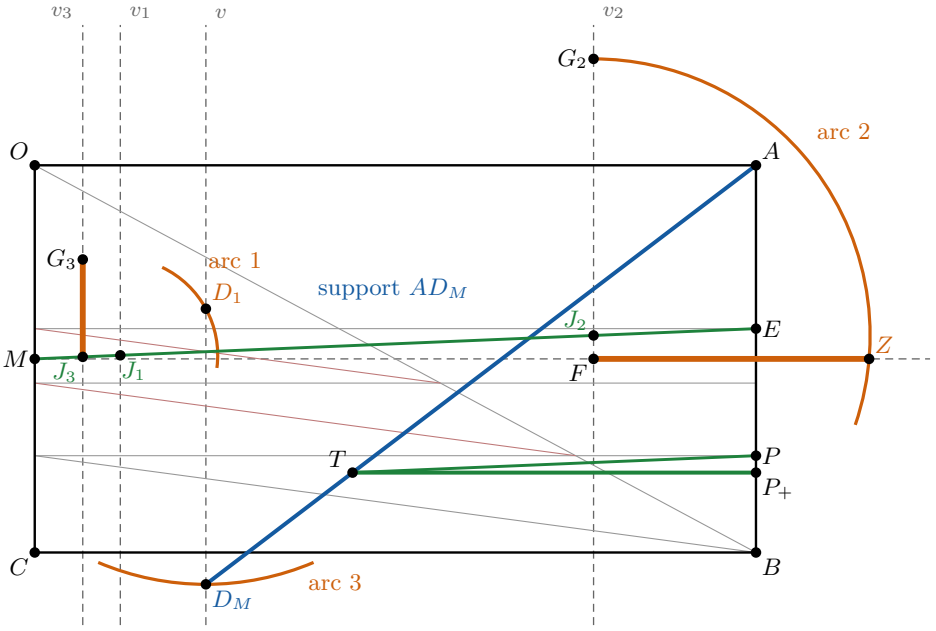



**Figure 4:** The three-mean support for $p = 3$, $X = 2$, $H = 4$, $s = 3/4$, with $W = 7.451\ldots$ from (5.4), drawn from the exact coordinates at equal axis scales. Dashed: prepared verticals and the horizontal through $M$. The free points $J_1, J_2, J_3$ are on the transport line $ME$ (green). The compass openings $J_3G_3$ and $FZ$ are the thick orange segments; the three arcs are orange; the support $AD_M$ is blue. Grey: the triangle chain.

*Positivity.* Clearing denominators gives the identity

$$\ell_M^2 - n^2 S_M = \frac{Q_0\,(\tau-1)^4 + Q_1\,\tau\,(\tau-1)^2 + Q_2\,\tau^2}{900\,p^2(4p^2-1)(5p^2+4)}, \tag{5.6}$$

with $Q_0 = (p-2)^2(2p-1)(313p^3+272p^2+200p+16)$, $Q_1 = 60\,p\,(p-2)(2p-1)(71p^3+74p^2+40p-8)$ and $Q_2 = 180\,p^2(149p^4+49p^3-141p^2-196p-20)$. For $p > 2$, $Q_0 \geq 0$, $Q_1 > 0$ and $Q_2 > 0$, the last because $149p^4+49p^3-141p^2-196p-20 = 149\varrho^4+1241\varrho^3+3729\varrho^2+4596\varrho+1800$ with $\varrho = p-2$. Hence $\ell_M^2 > n^2 S_M$, and as $\ell_M > 0$ we get $\ell_M > n\rho_M$: this is (i).

*The slope.* Let

$$\Lambda_M(\tau) = \log\bigl(\tau^2 + c\,q\bigr) - \log\bigl(1 + c\,q\bigr) - \frac{2}{p}\log\tau, \qquad \text{so that} \qquad -\Lambda_M(\sqrt{t}) = \frac{\log t}{p} + \log\frac{1 + c\,q_M}{t + c\,q_M} = e_+.$$

Both logarithms are defined by (i). Differentiating, with $q' = \ell'_M - nS'_M/(2\rho_M)$,

$$\tau\rho_M(\tau^2+cq)(1+cq)\,\Lambda'_M = 2\tau^2(1+cq)\rho_M + c\,\tau(1-\tau^2)\bigl(\ell'_M\rho_M - \tfrac{1}{2}nS'_M\bigr) - \tfrac{2}{p}(\tau^2+cq)(1+cq)\rho_M.$$

The right side is a cubic polynomial in $\rho_M$. Reducing it with $\rho_M^2 = S_M$ and substituting (5.1) gives

$$\Lambda'_M(\tau) = -\,\frac{(p^2-4)(p^2-1)\,\bigl(2\Psi_2\,\rho_M - 7\Psi_1\bigr)}{1800\,p^3(4p^2-1)^2(5p^2+4)^2\;\tau\;\rho_M\;(\tau^2+cq)(1+cq)}, \tag{5.7}$$

where $\Psi_1$ is a palindromic sextic and $\Psi_2$ a palindromic quartic in $\tau$ with coefficients in $\mathbb{Z}[p^2]$, listed in Table 4. Every factor of the denominator is positive.

*The sign.* The three coefficients of $\Psi_2$ in Table 4 are positive for $p > 2$, so $\Psi_2 > 0$ for $\tau > 0$. Rationalizing,

$$4\Psi_2^2\,S_M - 49\Psi_1^2 = \frac{4\,(4p^2-1)^3(5p^2+4)^2}{21\,p^2}\;(\tau-1)^8\;\Psi_3, \tag{5.8}$$

a polynomial identity after clearing $84p^2$, where $\Psi_3$ is a third palindromic quartic whose three coefficients are again positive. Let $\tau > 0$, $\tau \neq 1$. If $\Psi_1 \leq 0$ then $2\Psi_2\rho_M > 0 \geq 7\Psi_1$. Otherwise both sides are positive and (5.8) gives $(2\Psi_2\rho_M)^2 > (7\Psi_1)^2$. In both cases $2\Psi_2\rho_M > 7\Psi_1$, and by (5.7) $\Lambda'_M < 0$ for $\tau \neq 1$. The factor $(\tau-1)^8$ is the contact of order eight.

*Convergence.* $\Lambda_M$ is strictly decreasing and $\Lambda_M(1) = 0$, because $q(1) = 2m+g-n = 1$. Hence $e_+ = -\Lambda_M(\sqrt{t})$ has the sign of $t-1$, that is the sign of $e$: the state does not cross $\alpha$. Meanwhile $\mathrm{T}_M(s)/s-1 = (1-t)/(t+c\,q_M)$ moves the state toward $\alpha$. The orbit is monotone and bounded between $s_0$ and $\alpha$; its positive limit is a fixed point by continuity, and a fixed point has $t = 1$. This is (ii).

*Local order.* Both $q_M/\sqrt{t}$ and $q_*/\sqrt{t}$ are even analytic functions of $\log t$, hence power series in $w$, and exact expansion gives

$$\frac{q_M - q_*}{\sqrt{t}} = D_4^M\, w^4 + O(w^5), \qquad D_4^M = \frac{(2-h)(1+h)(2+h)(1-2h)(1+2h)(8h^2+17)}{203212800}. \tag{5.9}$$

Since $w = \xi^2/t$, $\kappa-\kappa_* = (p-1)D_4^M\xi^8+O(\xi^9)$, and Lemma 2.1 with $\omega = 8$ gives $e_+ = (p-1)p^7D_4^Me^9+O(e^{10})$, which is (5.5); oddness removes the term in $e^{10}$. In Lean the expansion (5.9) is obtained without Taylor series. Put $y = \frac{1}{2}\log t$, so that $\sqrt{t} = e^y$ and the conic radical is $e^y\sqrt{1+dw}$. If $R_4$ is the quartic Taylor polynomial of $\sqrt{1+dw}$, then $1+dw-R_4^2$ is $w^5$ times a polynomial, so replacing the radical by $e^yR_4(w)$ costs $O(w^5)$. After this replacement and after subtracting $D_4^Me^yw^4$, the difference with $q_*$, multiplied by $60(4-h^2)(4h^2+5)(1-h)(e^{2hy}-1)e^{8y}$, is a sum of 22 exponentials $c_j(h)e^{(k_j+2hl_j)y}$ whose moments $\sum_j c_j(k_j+2hl_j)^n$ vanish for $n < 11$; it is therefore $O(y^{11})$, and $w/y^2 \to 4$ gives $(q_M-q_*)/y^8 \to 256\,D_4^M$. □

**Table 4:** The certificate polynomials of Theorem 5.1. $\Psi_1$ is given by its coefficients on $\tau^6+1$, $\tau^5+\tau$, $\tau^4+\tau^2$, $\tau^3$; $\Psi_2$ and $\Psi_3$ by their coefficients on $(\tau-1)^4$, $\tau(\tau-1)^2$, $\tau^2$. Each coefficient of $\Psi_2$ and $\Psi_3$ is positive for $p > 2$: written in powers of $p-2$ it has nine positive coefficients.

| | | |
|---|---|---|
| $\Psi_1$ | $\tau^6+1$ | $1175p^8+2755p^6+2352p^4+880p^2+128$ |
| | $\tau^5+\tau$ | $5120p^8-3584p^6-3264p^4+1984p^2-256$ |
| | $\tau^4+\tau^2$ | $-6635p^8+13877p^6+17808p^4+1808p^2-128$ |
| | $\tau^3$ | $75776p^8-121856p^6+54912p^4-9344p^2+512$ |
| $\Psi_2$ | $(\tau-1)^4$ | $30185p^8+32563p^6+16572p^4+8032p^2+128$ |
| | $\tau(\tau-1)^2$ | $54180p^8+100044p^6+85680p^4+32256p^2$ |
| | $\tau^2$ | $262836p^8-335160p^6+310464p^4$ |
| $\Psi_3$ | $(\tau-1)^4$ | $489845p^8+647956p^6+361344p^4+123904p^2-1024$ |
| | $\tau(\tau-1)^2$ | $804380p^8+1583824p^6+2050176p^4+1033216p^2-4096$ |
| | $\tau^2$ | $3829896p^8-3081456p^6+2225664p^4+2128896p^2$ |

The proof has the structure of the proof of Theorem 3.1, one radical, one rationalization and one sign discussion, and not that of Theorem 4.4, whose two nested radicals required a two-region certificate with 345 terms: in the variable $\sqrt{t}$ three quartics suffice.

*Remark* 5.2 (Other members of the family; computer algebra). The same matching with fewer members gives lower orders. With A and one free conic mean,

$$q_7(t) = m_7\,(1+t) + n_7\sqrt{t-\varepsilon_7\,(t-1)^2}, \qquad m_7 = \frac{(h+3)(1-2h)}{4(4-h^2)}, \quad n_7 = \frac{5(1+h)}{2(4-h^2)}, \quad \varepsilon_7 = \frac{1-4h^2}{60},$$

has contact six: a single radical gives order seven, with $e_+ = -\frac{(p^2-1)(p^2-4)(4p^2-1)}{302400}e^7+O(e^9)$; for cube roots $q_7 = \frac{1}{14}(1+t)+\frac{6}{7}\sqrt{t-(t-1)^2/108}$. But the conic parameter is negative: the radicand is positive only for $w < 60/(1-4h^2)$, and the negative constant means that the state crosses the root at each step. The same happens for the combination of two free conic means, which has contact eight with one negative parameter. Imposing both A and G is what makes the third parameter $d$ positive in (5.2). These statements are exact series computations; no convergence theorem is claimed for $q_7$.

# 6 Geometric work: inventory, comparison and efficiency

Throughout this section $p \geq 3$ is an integer (or the numerator $\mu$ of a rational degree, Proposition 4.5), the state $R(s)$ is supplied, and counts follow Section 2.4. For every support the power stage uses $2p-1$ parallels and the join $L_1B$, and transport adds the join $ME$ and two parallels (the parallel through $P$ and the horizontal readout). The supports differ in what they add: nothing for MB and AK, whose support lines are prepared; one arc and one join for centered and decentered AD; two joins for projective AD; three arcs and one join for the three-mean support; and the arithmetic of Table 5 for the nested support.

## 6.1 Complete inventory of the nested support

Fixed preparation includes $a_9, b_9, c_9$ and $\lambda_9 = (p-1)/X$; every residual-dependent length is rebuilt at each step. Obtain $E = R(s^p)$ by the triangle stage, then $R(t)$ by the two-join fixed scale $X$. Stop if $t = 1$. Otherwise use

$$w = t + \frac{1}{t} - 2, \tag{6.1}$$

which needs one five-join division and two rail sums or differences instead of a separate squaring. Then construct successively

$$K = 1 + \frac{b_9 w}{1 + c_9 w}, \qquad k_9 = \sqrt{1 \cdot K}, \qquad \rho_9 = 1 + \frac{a_9 w}{k_9}, \qquad q_9 = \sqrt{t\,\rho_9}.$$

Each mean proportional uses the semicircle macro of Section 7.3, at most $2\mathsf{j} + \mathsf{p} + 3\mathsf{c}$ including diameter preparation and transfer to the rail. Scale $q_9$ to $\lambda_9 q_9$ in two joins; its rail length is $H\lambda_9 q_9$. One arc centred at $M$ transfers this length downward on the left rail and gives $D_9 = (0,\ H - \frac{H}{X}(1 + (p-1)q_9))$. Join $AD_9$ and $ME$, draw the parallel to $ME$ through $P$, and return horizontally.

**Table 5:** Per-step upper inventory of the nested support, from $R(s)$ to $R(s_+)$, integer $p \geq 3$. A sum or nonnegative difference is one rail arc, a general division five joins, a fixed scale two joins.

| Stage | j | p | c |
|---|---|---|---|
| Triangle power endpoint $E = R(s^p)$ | 1 | $2p-1$ | 0 |
| Residual $t = Xs^p$ | 2 | 0 | 0 |
| Width $w = t + 1/t - 2$ | 5 | 0 | 2 |
| Inner argument $K$ (two scales, one division, two sums) | 9 | 0 | 2 |
| First mean $k_9 = \sqrt{1 \cdot K}$ | 2 | 1 | 3 |
| Outer argument $\rho_9$ (scale, division, sum) | 7 | 0 | 1 |
| Second mean $q_9 = \sqrt{t\rho_9}$ | 2 | 1 | 3 |
| Scale $\lambda_9 q_9$ and transfer from $M$ to $D_9$ | 2 | 0 | 1 |
| Support join $AD_9$ | 1 | 0 | 0 |
| Join $ME$, transport parallel, horizontal readout | 1 | 2 | 0 |
| Total | 32 | $2p+3$ | 12 |

**Proposition 6.1** (Nested-radical work bound)**.** *For integer $p \geq 3$, $X > 0$ and a supplied state $R(s)$, the protocol above realizes the nested-radical correction with at most*

$$32\mathsf{j} + (2p+3)\mathsf{p} + 12\mathsf{c} = (4p+38)\mathsf{j} + (6p+21)\mathsf{c}, \tag{6.2}$$

*that is $10p + 59$ traces per nonterminal step; 89 traces for cube roots.*

*Proof.* The rail identities (2.2) establish every division and fixed scale. Both mean-proportional inputs are positive, and the prescribed circle intersection with the transferred length gives the positive root. The point $D_9$ gives $\kappa = 1 + (p-1)q_9$ in (2.3). Adding the ten rows gives the left side of (6.2), and $\mathsf{p} = 2\mathsf{j} + 3\mathsf{c}$ gives the right side. Unit shortcuts, reused objects and an exact-root stop can only reduce the count. □

If charged, the final inversion adds 5j once, and supplying $u_0$ instead of $s_0$ another 5j.

## 6.2 Inventory of the three-mean support

Fixed preparation consists of the four verticals $v, v_1, v_2, v_3$, the horizontal through $M$ and the points $F, G_2, G_3$ of Section 5.2, in a rectangle of the shape (5.4). The residual is not transferred to a rail: the line $ME$, drawn for the transport, carries it to the three verticals at no cost.

**Proposition 6.2** (Three-mean work bound)**.** *For integer $p \geq 3$, $X > 0$, a rectangle satisfying (5.4) and a supplied state $R(s)$, the protocol of Section 5.2 realizes the three-mean correction with at most*

$$3\mathsf{j} + (2p+1)\mathsf{p} + 3\mathsf{c} = (4p+5)\mathsf{j} + (6p+6)\mathsf{c}, \tag{6.3}$$

*that is $10p + 11$ traces per step; 41 traces for cube roots. In an arbitrary rectangle one more join suffices.*

**Table 6:** Per-step upper inventory of the three-mean support, from $R(s)$ to $R(s_+)$, integer $p \geq 3$.

| Stage | j | p | c |
|---|---|---|---|
| Triangle power endpoint $E = R(s^p)$ | 1 | $2p-1$ | 0 |
| Arc 1: centre $J_1$, opening $J_3G_3$, onto $v$ at $D_1$ | 0 | 0 | 1 |
| Arc 2: centre $J_2$ through $G_2$, onto the horizontal of $M$ at $Z$ | 0 | 0 | 1 |
| Arc 3: centre $D_1$, opening $FZ$, onto $v$ at $D_M$ | 0 | 0 | 1 |
| Support join $AD_M$ | 1 | 0 | 0 |
| Join $ME$, transport parallel, horizontal readout | 1 | 2 | 0 |
| Total | 3 | $2p+1$ | 3 |

*Proof.* Section 5.2 shows that the three arcs meet their lines at every state and that $AD_M$ has the slope $\frac{H}{WX}[1 + (p-1)q_M]$, so that (2.3) gives $\mathrm{T}_M$. The points $J_1, J_2, J_3$ and the two compass openings are intersections and distances of drawn or prepared objects, which are not charged. Adding the six rows gives the left side of (6.3), and $\mathsf{p} = 2\mathsf{j} + 3\mathsf{c}$ gives the right side. For the last assertion replace $J_1$ by the intersection of $v_1'$, the vertical at distance $K_n\sqrt{\zeta^2 - 1}$ from $v$, with the join of $E$ to a prepared centre chosen so that this intersection has the height $H - \frac{\lambda}{\gamma}[1 + (p-1)m(1+t)]$. □

The bound relies on the convention of Section 2.4 more than the other inventories do: it uses seven prepared objects and three free intersections where the decentered arc uses three prepared objects, and it prescribes the shape of the rectangle. The comparison with the nested inventory, which was written without such shortcuts, should be read with this in mind (Section 10).

## 6.3 Seven supports at a common state

**Table 7:** Mobile work per step with the triangle power stage, integer $p \geq 3$.

| Construction | Order | j | p | c | Traces | Scalar scope |
|---|---|---|---|---|---|---|
| MB rectangle | 1 | 2 | $2p+1$ | 0 | $10p+7$ | $X > 1$ |
| AK rectangle | 2 | 2 | $2p+1$ | 0 | $10p+7$ | global |
| AD rectangle | 3 | 3 | $2p+1$ | 1 | $10p+9$ | global |
| Projective AD | 4 | 4 | $2p+1$ | 0 | $10p+9$ | global |
| Decentered AD | 5 | 3 | $2p+1$ | 1 | $10p+9$ | global, $p > 2$ |
| Nested radicals | 9 | 32 | $2p+3$ | 12 | $10p+59$ | global, $p > 2$ |
| Three means | 9 | 3 | $2p+1$ | 3 | $10p+11$ | global, $p > 2$ |

For cube roots the per-step bounds are $37, 37, 39, 39, 39, 89, 41$. Table 8 runs all seven from the same state $X = 2$, $s_0 = 3/4$ (so $u_0 = 4/3$, not the $u_0 = 1$ of the illustration) with the same stopping test on the reciprocal relative error.

**Table 8:** Steps / summed trace bounds to reach $|s/\alpha - 1| \leq 10^{-d}$ for $p = 3$, $X = 2$, $s_0 = 3/4$. Each total is the per-step bound times the number of steps. Counts agree at 250 and 500 working digits.

| Construction | Order | $d = 6$ | $d = 12$ | $d = 30$ | $d = 60$ |
|---|---|---|---|---|---|
| MB rectangle | 1 | 8 / 296 | 17 / 629 | 44 / 1628 | 90 / 3330 |
| AK rectangle | 2 | 3 / 111 | 4 / 148 | 5 / 185 | 6 / 222 |
| AD rectangle | 3 | 2 / 78 | 3 / 117 | 3 / 117 | 4 / 156 |
| Projective AD | 4 | 2 / 78 | 2 / 78 | 3 / 117 | 3 / 117 |
| Decentered AD | 5 | 1 / 39 | 2 / 78 | 2 / 78 | 3 / 117 |
| Nested radicals | 9 | 1 / 89 | 1 / 89 | 2 / 178 | 2 / 178 |
| Three means | 9 | 1 / 41 | 1 / 41 | 2 / 82 | 2 / 82 |

For cube roots the nested support needs fewer steps but more traces than the decentered arc at every target in the table: $89, 89, 178, 178$ against $39, 78, 78, 117$. Higher order alone does not give a drawing-work advantage; the next subsection shows that for the nested support this is a statement about small $p$. The three-mean support takes the same numbers of steps as the nested support at 41 traces each: $41, 41, 82, 82$.

Against the decentered arc it wins at $d = 12$ and $d = 60$ and loses by a few traces at $d = 6$ and $d = 30$, where both need the same number of steps.

### 6.4 Efficiency index

For an iteration of order $\varrho$ costing $N$ units per step, the classical efficiency index is $\varrho^{1/N}$ [10, 9]: the number of correct digits is asymptotically multiplied by $\varrho^{1/N}$ per unit of work. We compare its logarithm $\iota = \log \varrho/N(p)$, with $N(p)$ the trace bound of Table 7.

**Proposition 6.3** (Efficiency ordering)**.** *For every integer $p \geq 3$, $\iota_{\mathrm{AK}} < \iota_{\mathrm{AD}} < \iota_{\mathrm{proj}} < \iota_{\mathrm{dec}}$. The nested support satisfies $\iota_{\mathrm{nest}} > \iota_{\mathrm{dec}}$ if and only if*

$$p > \frac{59 \log 5 - 9 \log 9}{10 \log(9/5)} = 12.79\ldots,$$

*that is, for integer degrees, if and only if $p \geq 13$. It exceeds $\iota_{\mathrm{AD}}$ from $p = 5$ and $\iota_{\mathrm{proj}}$ from $p = 8$. The three-mean support satisfies $\iota_M > \iota_{\mathrm{dec}}$ and $\iota_M > \iota_{\mathrm{nest}}$ for every $p > 0$: it has the largest index of the seven supports at every integer degree $p \geq 3$.*

*Proof.* The last three of the first group share $N = 10p + 9$ and have increasing orders, and $\log 2/(10p + 7) < \log 3/(10p + 9)$ because $10p \log(3/2) > 9 \log 2 - 7 \log 3$, whose right side is negative. The inequality $\log 9/(10p + 59) > \log 5/(10p + 9)$ is linear in $p$ and rearranges to the stated threshold; the comparisons with orders three and four give $p > 4.1$ and $p > 7.6$ in the same way. Finally $\log 9/(10p + 11) > \log 5/(10p + 9)$ reads $10p \log(9/5) > 11 \log 5 - 9 \log 9$, whose right side is negative because $5^{11} < 9^9$, and $\iota_M > \iota_{\mathrm{nest}}$ because the order is the same and $10p + 11 < 10p + 59$. □

**Table 9:** $10^3 \iota = 10^3 \log \varrho/N(p)$. The largest value in each column is in bold.

| Construction | $p = 3$ | 5 | 8 | 12 | 13 | 20 | 50 |
|---|---|---|---|---|---|---|---|
| AK | 18.73 | 12.16 | 7.97 | 5.46 | 5.06 | 3.35 | 1.37 |
| AD | 28.17 | 18.62 | 12.34 | 8.52 | 7.90 | 5.26 | 2.16 |
| Projective AD | 35.55 | 23.50 | 15.58 | 10.75 | 9.97 | 6.63 | 2.72 |
| Decentered AD | 41.27 | 27.28 | 18.08 | 12.48 | 11.58 | 7.70 | 3.16 |
| Nested radicals | 24.69 | 20.16 | 15.81 | 12.27 | 11.63 | 8.48 | 3.93 |
| Three means | **53.59** | **36.02** | **24.15** | **16.77** | **15.58** | **10.41** | **4.30** |

The reason is visible in Table 7: the power stage costs about $10p$ traces for every support, so the 50 additional traces of the nested support are a fixed overhead that large $p$ amortizes, and the ratio of indices tends to $\log 9/\log 5 \approx 1.37$. The three-mean support has an overhead of two traces only, so it leads at every degree: the ratio of its index to that of the decentered arc is 1.30 at $p = 3$ and tends to the same limit. The index is an asymptotic quantity built from upper inventories; at a finite accuracy the integer number of steps makes the comparison lumpy, as Table 10 shows.

**Table 10:** Steps / summed trace bounds for $p = 20$, $X = 2$, $s_0 = 3/4$ (per-step bounds 209, 259 and 211).

| Construction | $d = 30$ | $d = 60$ | $d = 250$ | $d = 1000$ | $d = 2500$ |
|---|---|---|---|---|---|
| Decentered AD | 4 / 836 | 5 / 1045 | 5 / 1045 | 6 / 1254 | 7 / 1463 |
| Nested radicals | 3 / 777 | 3 / 777 | 4 / 1036 | 5 / 1295 | 5 / 1295 |
| Three means | 3 / 633 | 3 / 633 | 4 / 844 | 4 / 844 | 5 / 1055 |

At $p = 20$ the nested support has a smaller total than the decentered arc at four of the five targets and loses at $d = 1000$, where saving a single step (five instead of six) does not pay for the higher step cost. The three-mean support has the smallest total at every target of the table.

## 7 Direct root enclosures for real degrees

The power stage can be avoided altogether by constructing the root directly. The input is a positive length $X$ and a real degree $p$, also given as a length; the output is an approximation of $r = X^{1/p}$ with prescribed

relative error. A real input length is assumed to be available: this does not assert that every real number is constructible from a unit segment. This calculator is the only one in the paper whose every step is a finite construction for irrational $p$. We first treat $X > 1$ and $p \geq 1$; the cases $X = 1$ and $p = 1$ are immediate, and Proposition 7.2 removes both restrictions.

## 7.1 One mean proportional per subdivision

Set $\theta = 1/p$, $a = 1$, $b = X$ and $\lambda = \theta$. Here $a, b$ are moving rail values. The invariant is

$$0 < a < b, \qquad 0 \leq \lambda \leq 1, \qquad r = a^{1-\lambda} b^{\lambda}. \tag{7.1}$$

If $\lambda \in \{0, 1\}$ return the corresponding endpoint, which is exact. Otherwise construct $m = \sqrt{ab}$ with the classical mean-proportional semicircle [4] and replace

$$(a, b, \lambda) \longmapsto \begin{cases} (a,\ m,\ 2\lambda), & \lambda \leq \frac{1}{2}, \\ (m,\ b,\ 2\lambda - 1), & \lambda > \frac{1}{2}. \end{cases} \tag{7.2}$$

Both branches preserve (7.1). Thus $p$ determines the choices and the weight, never the length of a power chain. After $n$ subdivisions

$$\frac{b}{a} = X^{2^{-n}}, \qquad z := \frac{b}{a} - 1 \geq 0. \tag{7.3}$$

No logarithm, exponential or power $s^p$ is evaluated. The branch test compares two constructed lengths, $\lambda$ and $\frac{1}{2}$; for irrational $p$ equality never occurs, and for dyadic $1/p$ the process stops with an exact endpoint.

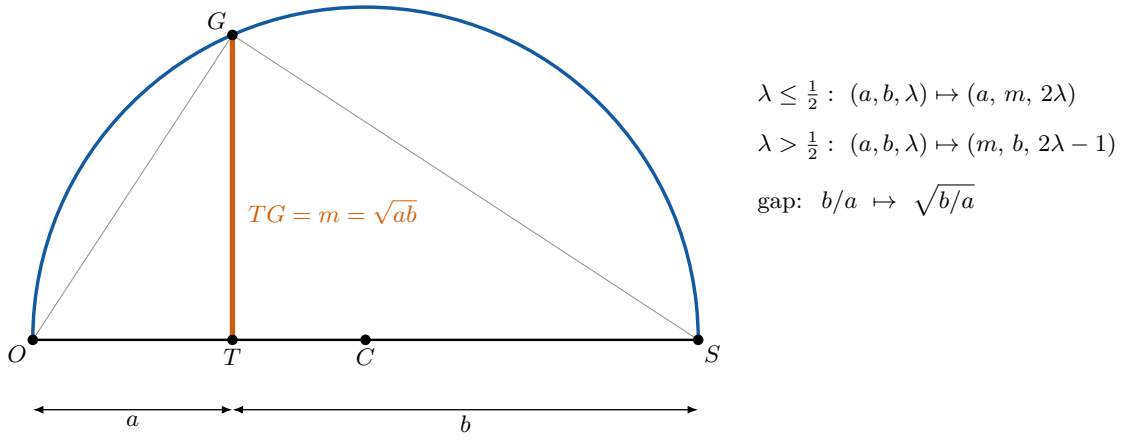



**Figure 5:** A subdivision constructs one mean proportional. The semicircle has diameter $OS = a + b$, centre $C$ and junction $OT = a$; the orange perpendicular $TG$ is the mean $m$. The same device is rotated onto the vertical rail in the counted protocol. The figure uses $a = 1.2$, $b = 2.8$ only to show the incidence.

## 7.2 A fifth-order final enclosure

The harmonic–arithmetic readout of the companion gallery [5], $L_2 = ab/[(1-\lambda)b + \lambda a]$ and $U_2 = (1-\lambda)a + \lambda b$, encloses $r$ by the weighted arithmetic–geometric mean inequality, with

$$\frac{U_2}{L_2} - 1 = \lambda(1-\lambda)\frac{z^2}{1+z} \leq \sinh^2\!\Big(\frac{\log X}{2^{n+1}}\Big),$$

a width quadratic in $z$. A single rational readout of degree two gives a fifth-order width. It is the diagonal [2/2] Padé approximant of $(1+z)^{\tau}$ at zero [6, 7]. For $0 \leq \tau \leq 1$ put

$$\Pi_{\tau}(z) = 12 + 6(2+\tau)z + (\tau+1)(\tau+2)z^2, \qquad \psi_{\tau}(z) = \frac{\Pi_{\tau}(z)}{\Pi_{-\tau}(z)}, \tag{7.4}$$

whose denominators are positive for $z \geq 0$, and

$$L_5 = a\,\psi_{\lambda}(z), \qquad U_5 = \frac{b}{\psi_{1-\lambda}(z)}. \tag{7.5}$$

**Proposition 7.1** (Enclosure and finite termination)**.** *For $X \geq 1$, real $p \geq 1$ and every subdivision depth,*

$$L_5 \leq X^{1/p} \leq U_5, \qquad \frac{U_5}{L_5} - 1 = \frac{\lambda(1-\lambda)(2-\lambda)(1+\lambda)\, z^5}{\Pi_\lambda(z)\, \Pi_{1-\lambda}(z)} \leq \frac{z^5}{256}. \tag{7.6}$$

*Given $\varepsilon > 0$, choose a positive rational $\beta$ with $\beta^5/256 \leq \varepsilon$, stop when $b \leq (1+\beta)a$ and return $L_5$. The procedure terminates and its relative error is at most $\varepsilon$. A sufficient depth depends on $X$ and $\varepsilon$ only, not on $p$.*

*Proof.* For $0 \leq \tau \leq 1$, direct differentiation gives

$$(1+z)\big(\Pi'_\tau \Pi_{-\tau} - \Pi_\tau \Pi'_{-\tau}\big) - \tau\, \Pi_\tau \Pi_{-\tau} = -\tau(1-\tau^2)(4-\tau^2)\, z^4 \leq 0.$$

Hence $\log \psi_\tau(z) - \tau \log(1+z)$ is nonincreasing from zero, so $\psi_\tau(z) \leq (1+z)^\tau$. With $\tau = \lambda$ this is $L_5 \leq r$; with $\tau = 1-\lambda$ and $(1+z)^\lambda (1+z)^{1-\lambda} = 1+z$ it is $r \leq U_5$. Multiplying out gives the equality in (7.6). With $\chi = \lambda(1-\lambda) \leq \frac{1}{4}$ the numerator coefficient is $\chi(2+\chi) \leq \frac{9}{16}$, and $\Pi_\lambda, \Pi_{1-\lambda} \geq 12$, so the width is at most $z^5/256$. At the stopping test $0 \leq z \leq \beta$, so $r/L_5 - 1 \leq \varepsilon$ and $(r - L_5)/r \leq \varepsilon/(1+\varepsilon)$. By (7.3), $z \to 0$, so the test is eventually met; any $n$ with $2^n \log(1+\beta) \geq \log X$ suffices. Equivalently $X \leq (1+\beta)^{2^n}$, which can be checked in exact rational arithmetic for rational input. □

It suffices to draw $L_5$ alone; the analytic upper bound certifies its accuracy without constructing a second Padé quotient. For $0 < X < 1$, constructing and inverting this lower bound for $1/X$ gives an upper approximation of the original root with relative error at most $\varepsilon$. The width is of order five in the rail gap $z$; this is not a fifth-order iteration, since each subdivision only halves the logarithmic gap.

**Proposition 7.2** (Every nonzero real degree and every positive input)**.** *Let $p \neq 0$ be real and $X > 0$, $X \neq 1$.*

*(i) If $X > 1$ and $0 < p < 1$, let $k = \lfloor 1/p \rfloor \geq 1$ and start from $a = X^k$, $b = X^{k+1}$, $\lambda = 1/p - k$. Then (7.1), (7.3) and Proposition 7.1 hold unchanged.*

*(ii) If $0 < X < 1$, apply the construction to $1/X$ and invert: the enclosure $[1/U_5, 1/L_5]$ has the same relative width.*

*(iii) If $p < 0$, apply the construction to $|p|$ and invert the output.*

*Proof.* In (i), $a^{1-\lambda} b^\lambda = X^{k+\lambda} = X^{1/p}$, $0 \leq \lambda < 1$ and $b/a = X$, so the invariant and the gap formula are those of the case $p \geq 1$, and the proof of Proposition 7.1 uses nothing else. Inversion maps an enclosure $[L, U]$ to $[1/U, 1/L]$ with the same ratio. □

## 7.3 A complete, conservative drawing inventory

Use the extended vertical rail $R(q)$, its origin $R(0)$ and the prepared centres of Section 2.2; $X$ and $p$ are given on the rail. The macros are:

- *Sum or nonnegative difference* of two rail values: one compass arc on the rail.
- *Product or quotient*: five joins (Section 2.2); by a prepared constant, two joins.
- *Mean proportional*, $2\mathsf{j} + \mathsf{p} + 3\mathsf{c}$: form $R(a+b)$ with one arc and $R((a+b)/2)$ with the two-join fixed scale; draw the semicircle through $R(0)$; draw the horizontal through $R(a)$ with one parallel macro; transfer the resulting length to the rail with one arc.

The updated weight uses the fixed scale $2\lambda$ and, on a right branch, one subtraction. A subdivision with its weight update costs at most $4\mathsf{j} + \mathsf{p} + 4\mathsf{c}$, and a stopping test, which scales $a$ by the prepared $1+\beta$, two joins. For the final readout use

$$L_5 = a\Big(1 + \lambda\, \frac{6z(2+z)}{\Pi_{-\lambda}(z)}\Big), \qquad \Pi_{-\lambda}(z) = 12 + 6(2-\lambda)z + (1-\lambda)(2-\lambda)z^2. \tag{7.7}$$

One evaluation schedule uses seven general products, namely $(1-\lambda)(2-\lambda)$, $z^2$, $(2-\lambda)z$, $(1-\lambda)(2-\lambda)z^2$, $z(2+z)$, the weighted quotient and the final scaling by $a$; two divisions, including $b/a$; two fixed scalings by 6; and seven sums or differences. Its cost is at most $49\mathsf{j} + 7\mathsf{c}$.

**Table 11:** Trace inventory of the direct enclosure for $X > 1$, $p \geq 1$.

| Operation | j | p | c |
|---|---|---|---|
| Initial weight $\lambda = 1/p$ | 5 | 0 | 0 |
| $n$ subdivisions and weight updates | $4n$ | $n$ | $4n$ |
| At most $n+1$ stopping tests | $2n+2$ | 0 | 0 |
| One final lower Padé readout | 49 | 0 | 7 |
| Total, parallels expanded | $8n+56$ | 0 | $7n+7$ |

Thus $15n + 63$ traces suffice for $X > 1$, $p \geq 1$. The other cases of Proposition 7.2 add: $5k + 1$ traces in case (i), for the $k$ products $X^2, \ldots, X^{k+1}$ and the difference $1/p - k$; two five-join inversions in case (ii), giving $15n + 73$ for $0 < X < 1$, $p \geq 1$; one five-join inversion in case (iii). Finding $k$ is a decision and is not charged. Constructing both endpoints $L_5$ and $U_5$ would require additional work and is not included in this single-output count.

## 7.4 Depth, precision and comparison with the iterations

**Table 12:** Sufficient depths at $X = 2$, uniformly in real $p \geq 1$. The Padé depths use $\beta = 19/100,\ 3/40,\ 3/250,\ 3/1000$; the inequalities $\beta^5/256 \leq \varepsilon$ and $(1+\beta)^{2^n} \geq 2$ verify them in rational arithmetic.

| Relative width target | Harmonic–arithmetic depth | Padé depth | Trace bound $15n + 63$ |
|---|---|---|---|
| $10^{-6}$ | 9 | 2 | 93 |
| $10^{-8}$ | 12 | 4 | 123 |
| $10^{-12}$ | 19 | 6 | 153 |
| $10^{-15}$ | 24 | 8 | 183 |

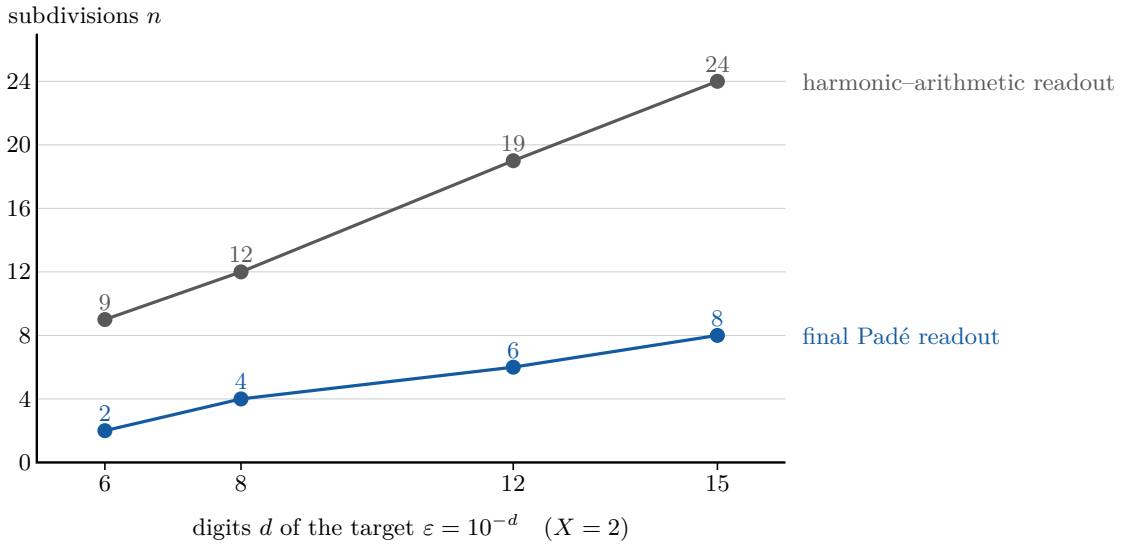



**Figure 6:** Sufficient worst-case depths of Table 12, uniformly in $p \geq 1$. Points are verified depth certificates; the connecting segments only guide the eye and do not represent fractional subdivisions.

For $p = 37.5$, four subdivisions yield $a = 1$, $b = 2^{1/16}$ and $\lambda = 32/75$, and the root lies between 1.0186558096 and 1.0186558103; these rounded endpoints can be checked exactly by raising them to the power 75 and comparing with 4. At $X = 2$ and $\varepsilon = 10^{-8}$ the construction has the bound $88\mathsf{j} + 35\mathsf{c} = 123$ traces.

**When to use which calculator.** The subdivision gains a fixed number of bits per step, the iterations multiply the number of correct digits. For cube roots of 2, the depths needed for width $10^{-d}$ with $d = 6, 12, 30, 60$ are $n = 2, 6, 18, 38$, that is $93, 153, 333, 633$ traces, against $39, 78, 78, 117$ for the decentered arc and $41, 41, 82, 82$ for the three-mean support in Table 8. (The two columns are not the same quantity: a

guaranteed width on one side, an observed error on the other.) For small integer or rational degrees and high accuracy the iterations are cheaper; for irrational degrees, and for rational degrees with a large numerator, the subdivision is the calculator to use (Remark 4.8).

# 8 Attribution and algebraic approximation

High local order and geometric iteration are not new principles. Traub organizes classical iteration formulas and their error terms [8, 9]. Gander discusses Halley's method and radical corrections [11]; Scavo and Thoo analyze its geometry [12]. Melman connects geometry with global convergence, and Amat, Busquier and Gutiérrez develop geometric constructions for nonlinear iteration [13, 14]. Here AK is Newton under inversion and centered AD is Halley, realized in the shared rectangle; their scalar formulas are classical. Reading all supports as approximations of one function $\kappa_*$ (Lemma 2.1) is the usual principle that the order of an iteration is the order of contact of its iteration function with the exact one, specialized to the rectangle.

The decentered and nested supports are algebraic corrections defined by explicit positive radicals. Algebraic approximants generalize rational approximation and form an established methodology [3, 15]; the two-radical coefficient matching of Section 4 belongs to it. Section 4.6 proves a degree-four distinction at the cubic specialization, and Appendix C gives a specified quadratic comparison for the decentered support. The subdivision mean proportional is Euclid's [4]; its final readout is an ordinary Padé approximant [6, 7], with the enclosure and width proved in Section 7. Counting particular constructions follows the concerns of géométrographie and nomography [16, 17], and the efficiency index is Ostrowski's [10].

The three-mean support is a linear combination of three members of the family $q^2 = t + a(t-1)^2$, and its method is not new either. Since $q_*$ is a homogeneous mean of 1 and $t$, the support belongs to a classical subject, the approximation and bounding of means such as the logarithmic and extended means by combinations of the arithmetic, geometric and quadratic means [25, 26]. Its coefficient matching is of Padé type in a wider sense: in the variable $w$ it is a quadrature rule for the kernel $\sqrt{1+aw}$ with two prescribed nodes, in the way ordinary Padé approximants of Stieltjes series are Gaussian quadratures for the kernel $1/(1+aw)$ [7]; and in the variable $\sqrt{t}+1/\sqrt{t}$ it is a quadratic algebraic approximant subject to one constraint (Appendix C). Raising the order of a root iteration by an affine combination of known iterations is also an established device, used for $n$th roots with rational iterations in [27].

What this paper contributes is the stated rectangle realizations, their domains, the scalar convergence proofs with explicit constants, the protocol bounds, and the classification of degrees.

# 9 Evidence and reproducibility

**Lean.** The nested-radical results have two project Docker/Lean audits totalling 104 theorems: 38 cubic, 14 real-parameter certificates, 44 real-parameter analysis and 8 degree-extension theorems. They use only `propext`, `Classical.choice` and `Quot.sound`, with no admitted proof. The sources, pinned toolchain, hashes and audit records accompany the paper [18, 19, 20]. The four nested-radical modules are those of V27-NR; for V28 they were recompiled from source in a separate environment (Lean 4.33.1, Mathlib v4.33.1, Mathlib itself built from source), the count of 104 theorems was confirmed, and the main theorems (global convergence, the extension to every nonzero degree and the cubic limit) were checked to depend on these three axioms only. V28 added six modules, 125 theorems in all, with the same axioms and no admitted proof.

- `DecenteredArcGlobal` (30): Theorem 3.1, global monotone convergence of the decentered arc for every real $p > 2$, by the sign argument of Section 3.
- `ContactLimit` (12): Lemma 2.1 in limit form, and the analytic tool used for the local orders: a finite sum $\sum_j c_j e^{\lambda_j x}$ whose first $N$ moments $\sum_j c_j \lambda_j^n$ vanish is $O(x^N)$.
- `NestedOrderNine` (21): Theorem 4.1, the limit $\hat{e}_+/\hat{e}^{\,9} \to c_9(p)$ for every real $p > 2$. The expansion (4.6) of $Y$ through $w^4$ is an exponential sum of 27 terms with twelve vanishing moments; the nested radical is expanded algebraically and the result is identified with (4.9).
- `ArcOrderFive` (10): the fifth-order limit (3.2) with its constant.

**Table 13:** Status of each claim. "Lean": checked by the Lean kernel, in the environments described below. "CAS": exact identity between polynomials or rational functions, recomputed with a computer-algebra system. "Numerical": high-precision evaluation, not a proof.

| Claim | Domain | Status |
|---|---|---|
| Lemma 2.1, Table 3 | analytic supports | Lean (limit form); constants of AK, AD and projective AD: CAS |
| Theorem 3.1 | real $p > 2$ | Lean (global convergence and the fifth-order limit); $O(e^7)$ remainder written |
| Theorem 4.1 | real $p > 2$ | Lean (limit $\hat{e}_+/\hat{e}^{\,9} \to c_9(p)$, positivity, $c_9(3)$); $O(\hat{e}^{\,11})$ remainder written |
| Theorem 4.3 | $p = 3$, $X > 0$ | Lean |
| Theorem 4.4 | real $p > 2$ | Lean; certificate structure also CAS |
| Theorem 5.1 | real $p > 2$ | Lean (positivity, global convergence, the limit $e_+/e^9 \to c_M(p)$, positivity of $c_M$, $c_M(3)$); identities also CAS; $O(e^{11})$ remainder written |
| Remark 5.2 | real $p > 2$ | CAS (exact series) |
| Proposition 4.5 | rational $p$ | Lean, for the three radical supports |
| Proposition 4.6 | real $p \neq 0$ (scalar) | Lean |
| Proposition 4.7 | real $p > 0$ | Lean |
| Proposition 6.1 | integer $p \geq 3$ | written inventory; totals Lean; incidence checks |
| Proposition 6.2 | integer $p \geq 3$ | written inventory; total Lean; incidence simulation |
| Proposition 6.3, Table 9 | real and integer $p \geq 3$ | Lean; table values numerical |
| Tables 8, 10 | stated examples | numerical |
| Proposition 7.1 | $X \geq 1$, $p \geq 1$ | written proof; scalar part in Lean (retained) |
| Proposition 7.2 | real $p \neq 0$, $X > 0$ | Lean (invariant, gap, inversion) |
| Degree four (Section 4.6) | $p = 3$, $t = 2$ | exact rational computation |
| Appendix C, three-mean paragraph | $p = 3$ | exact rational computation (series only) |

- `DegreesEfficiency` (47), depending on Mathlib only: the exact contact identity; the positivity of $N_9$ and $c_9$, $c_9(3) = 7/648$ and $c_9(p) = \frac{1}{2}(p-1)p^7 D_4(1/p)$; Propositions 4.7 and 6.3, including $12 <$ crossover $< 13$ from $9^{129} < 5^{179}$ and $5^{189} < 9^{139}$; the trace totals of Section 6; the invariant of Proposition 7.2.
- `DegreesNested` (5): Proposition 4.5 for the nested support and for the decentered arc, without hypothesis and with integer powers only.

This revision adds three modules for the three-mean support, 93 theorems in all, compiled in the project Docker environment (Lean 4.33.1, Mathlib v4.33.1), with no admitted proof and no warning; their main theorems were checked to depend on the same three axioms only.

- `ThreeMeanGlobal` (57): parts (i) and (ii) of Theorem 5.1 for every real $p > 2$, in the variable $\sqrt{t}$: the identities (5.6), (5.7) and (5.8), the positivity of the nine certificate polynomials, the enclosure of the correction between 1 and $t^{1/p}$, global convergence, and the agreement of the Lean definition with (5.2).
- `ThreeMeanOrderNine` (29): part (iii), the limit $\hat{e}_+/\hat{e}^{\,9} \to c_M(p)$ for every real $p > 2$, with $c_M > 0$ and $c_M(3) = 23/20736$. The radical is replaced by its quartic Taylor polynomial at an exact algebraic cost, and the remaining exponential sum has 22 terms and ten vanishing moments (the tool of `ContactLimit`).
- `ThreeMeanWork` (7): the total $10p + 11$ of Table 6; the inequalities $\iota_M > \iota_{\mathrm{dec}}$ and $\iota_M > \iota_{\mathrm{nest}}$ for every $p > 0$, the first from $5^{11} < 9^9$; and Proposition 4.5 for the three-mean support.

The local orders are stated as limits of $e_+/e^{\omega+1}$; the refinements $O(e^7)$ and $O(e^{11})$ of the remainders, which follow from oddness, are written arguments.

| Lean module | Certified scope |
|---|---|
| `NestedRadicalCubic` | Cubic global convergence and the relative-error limit 7/648, for every positive target. |
| `NestedRadicalRealCertificate` | Exact polynomial identities and positive-coefficient certificates. |
| `NestedRadicalReal` | Original formula for every real $p > 2$; support equivalence and the small-degree counterexample. |
| `NestedRadicalAllDegrees` | Degree doubling, preservation of the reported start and convergence for every $p \neq 0$. |
| `DecenteredArcGlobal` | New in V28: global convergence of the decentered arc, real $p > 2$. |
| `ContactLimit` | New in V28: contact lemma in limit form; exponential sums with vanishing moments. |
| `NestedOrderNine` | New in V28: order nine with constant $c_9(p)$ for every real $p > 2$. |
| `ArcOrderFive` | New in V28: order five of the decentered arc with its constant. |
| `DegreesEfficiency` | New in V28: contact identity, constants, irrational degrees, efficiency ordering and crossover, trace totals, subdivision start for every positive degree. |
| `DegreesNested` | New in V28: rational degrees for the decentered and nested iterations. |
| `ThreeMeanGlobal` | New in V29: positivity and global convergence of the three-mean support, real $p > 2$. |
| `ThreeMeanOrderNine` | New in V29: order nine of the three-mean support with constant $c_M(p)$. |
| `ThreeMeanWork` | New in V29: trace total, efficiency inequalities and rational degrees for the three-mean support. |
| `GeometricSubdivision` | Scalar interval invariant, real-degree rational bracket and width; stored seven-declaration audit, not recompiled for this revision [21]. |

**Computer algebra and numerics.** The accompanying script `verify_v29.py` recomputes, with exact rational arithmetic: the identities (3.3) (at sample points), (3.4), (4.10); the series (4.6)–(4.9) and the constants of Table 3; the positivity of $N_9(2+\rho)$; the factorization defining $\mathcal{P}$ in Theorem 4.4, its degrees, and the positivity and term counts 345, 49, 24, 112 of the four certificates; the Padé identity and the width equality (7.6); and the appendix formulas. Numerically it checks (4.16) against a numerical derivative, the constant $c_9(p)$ against the iteration at $p = 2.5, 3, 4, 7, 20$, the monotone enclosure $\min(u, r) < F_{p,X}(u) < \max(u, r)$ on a grid $p \in [2.001, 10^4]$, $t \in [10^{-12}, 10^{12}]$, and regenerates Tables 8, 9, 10 and 12 (working precision 300 to 2600 digits). For the three-mean support it recomputes exactly, and independently of Lean: the coefficient identities; (5.6), (5.7) and (5.8) with the positivity of the nine certificate polynomials; the series (5.9) with symbolic $h$ and the constant $c_M$; the series of Remark 5.2; and the rational computation of Appendix C. Numerically it checks (5.7) against a numerical derivative, the limit $e_+/e^9 \to c_M(p)$ at $p = 2.5, 3, 4, 7, 20$, the enclosure $\min(1, t^{1/p}) < \Gamma < \max(1, t^{1/p})$ on 7200 points with $p \in [2.001, 10^4]$ and $t \in [10^{-12}, 10^{12}]$, and the protocol of Section 5.2: the line and circle incidences are evaluated at 60 digits for 120 configurations ($p$ from 3 to 20, four inputs, five states), with the shape condition (5.4) and, with one more join, without it, and return the scalar update.

**Checks retained from V27.** The nested verifier checks coefficient identities, the cubic positive certificate, the degree-four specialization, eight exact local series and 80 residual probes at 140 digits. The illustrative first step is checked at 110 digits without using the cube root to place points. The nested inventory has 64 exact rational macro checks and 60 full line/circle evaluations at 160 digits, including support placement and report; four additional root-stop cases are checked. The subdivision verifier checks three exact polynomial identities, 188 rational rail incidences, four rational depth certificates, the outward-rounded $p = 37.5$ example and 256 numerical enclosures at 100 digits [21]. The complete source package contains `build.sh`, `verify.py`, the independent comparison script and validation records. Finite numerical probes supplement proofs and do not certify rounded implementations. The gallery contains companion interactive views; it does not certify finite drawing error.

**Figures.** All figures are generated by `genfigs.py` from the formulas of the paper; the script asserts, for each drawing, that the constructed point $P_+$ agrees with the scalar update to $10^{-12}$.

# 10 Scope and limits

The following limits apply to the whole paper and are stated here once.

1. **Approximation.** Every calculator produces a convergent sequence or a finite enclosure. No root is claimed to be exactly constructible in finitely many operations.
2. **Finite steps.** The fast iterations are finite constructions for integer and rational degrees only, at a cost governed by the numerator $\mu$. For irrational $p$ the convergence theorems are scalar statements; the geometric calculator is the subdivision.
3. **Counts.** Trace counts are upper bounds for the specified protocols under the convention of Section 2.4, which does not charge fixed preparation or decisions and weighs a join and an arc equally. They are not minimal, and they are not times, energies or drawing sizes. They are written inventories, not a formal cost semantics. The inventories do not use the convention to the same extent: the three-mean protocol takes its moving centres and compass openings from free intersections with seven prepared objects and prescribes the shape of the rectangle, whereas the nested protocol rebuilds every length on a rail.
4. **Efficiency.** The index of Proposition 6.3 is asymptotic and inherits the previous limit; a shorter nested protocol would lower the crossover degree 13, and a stricter convention on preparation would raise the cost of the three-mean support.
5. **Real drawings.** Exact incidences, the scalar real iteration and a physically inaccurate drawing are different objects. Conditioning, finite drawing error and floating-point behaviour are not analysed.
6. **Priority.** We have not identified the decentered, nested or three-mean formulas with a prior formula, but a bounded comparison cannot establish priority, and different explicit formulas may be equivalent under changes of variable (Appendix C).
7. **Formalization.** Lean covers exactly the entries so marked in Table 13. The convergence theorems of the three radical supports and their local orders are formalized. Not formalized: the constants of the classical supports in Table 3, the higher-order remainders, Remark 5.2, the degree-four computation of Section 4.6 and Appendix C. For the inventories Lean checks the arithmetic of the totals, not the geometric protocols.

# 11 Conclusion and open questions

Changing one line in the Pandrosion rectangle moves the iteration from order two to order nine, and the order is read off the contact of that line's slope with a single function $\kappa_*$. Three radical supports extend the classical ones: a decentered arc of order five at the mobile cost of Halley's construction, and two supports of order exactly nine for every real $p > 2$, both globally monotone: the nested radicals, with constant $c_9(p)$, and the three means, with the smaller constant $c_M(p)$ and a mobile cost of three arcs and one join. In trace counts, under the stated conventions, the three-mean support has the largest efficiency index at every degree $p \geq 3$; between the two others the decentered arc leads for $p \leq 12$ and the nested support for $p \geq 13$. These iterations are finite constructions for rational degrees; for a general real degree the power-free subdivision with a Padé readout gives a certified enclosure of relative width at most $z^5/256$ in $15n + 63$ traces.

Open questions:

1. Formalize a cost semantics for the drawing protocols, so that the inventories, and not only their totals, are machine-checked, and so that prepared objects can be weighed.
2. Shorten the nested inventory. Its overhead over the decentered arc is 50 traces, of which 19 build the two arguments $K$ and $\rho_9$ and 20 the two mean proportionals. The three-mean support shows that order nine does not require this overhead; whether the nested formula itself has a short protocol is open.
3. The family of Section 5 gives order seven with a single radical (Remark 5.2), but on a bounded range of residuals and with a state that crosses the root. Is there a single-radical support of order greater than five that is defined and monotone for every $t > 0$? Which order do three conic means, or four, reach with positive radicands?
4. Analyse the two-level recursion in which the residual $u^p$ of an irrational degree is itself enclosed by subdivision: which inner accuracy preserves the outer order?
5. Analyse conditioning and finite drawing error.

6. Compare the exact formulas with earlier algebraic approximants and with the literature on means under specified transformations.
7. Extend to the three-mean support the half-plane contraction proved for the decentered arc in the complex companion [28]. Numerically the boundary criterion of that paper holds for $p$ from 2.0001 to $10^4$, with $\sup_y \operatorname{Arg}\varphi(iy)\,p/\pi \approx 0.503$ against the bound 1; this is an observation, not a proof.

# A Classical rectangle supports

## A.1 AK and centered AD: orders two and three

*AK: a fixed line.* Prepare $K = (W(1 - X/p), 0)$. The support $AK$ has slope $Hp/(WX)$, so $\kappa = p$ and $\mathrm{T}_{\mathrm{AK}}(s) = ps/(p - 1 + t)$, Newton's method under inversion. It has order two and converges from every positive start.

*AD: a centered length transfer.* Prepare

$$O_{\mathrm{AD}} = \Big(W - \frac{2W}{p-1},\ H - \frac{H(p+1)}{X(p-1)}\Big).$$

Transfer $AE = Hs^p$ downward from this centre to $D_{\mathrm{AD}}$ and join $AD_{\mathrm{AD}}$. Then $\kappa = \frac{1}{2}[p+1+(p-1)t]$, giving

$$\mathrm{T}_{\mathrm{AD}}(s) = s\,\frac{p+1+(p-1)t}{p-1+(p+1)t}. \tag{A.1}$$

This Halley map has cubic order and global monotone convergence. Earlier geometric interpretations appear in [11, 12]; here the rail encoding and readout are shared with AK.

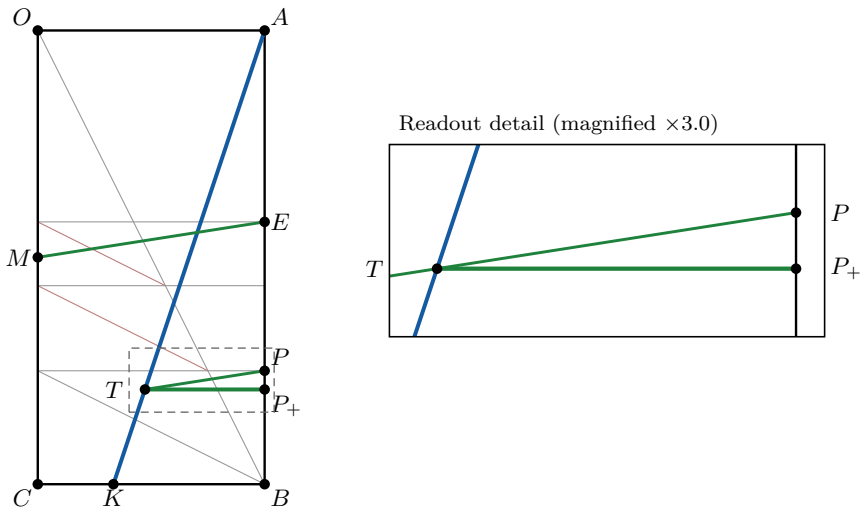



**Figure 7:** Pandrosion AK, order two, at $p = 3$, $X = 2$, $s = 3/4$ ($W = 2$, $H = 4$). The fixed support $AK$ (blue) replaces the MB support, while the triangle chain (grey) and the correction direction (green) are retained. The inset magnifies the dashed window around $P$, $T$ and $P_+$.

Both drawings retain the triangle stage, the green transport and the horizontal readout; only the support changes.

## A.2 Projective AD: order four

Two joins supply the support. Prepare the horizontal line and the point

$$\ell:\ y = H\Big(1 + \frac{5p-1}{(p+1)X}\Big), \qquad Z_{\mathrm{proj}} = \Big(W\Big(1 + \frac{5p-1}{2p(2p-1)}\Big),\ H\Big(1 + \frac{p+1}{(2p-1)X}\Big)\Big).$$

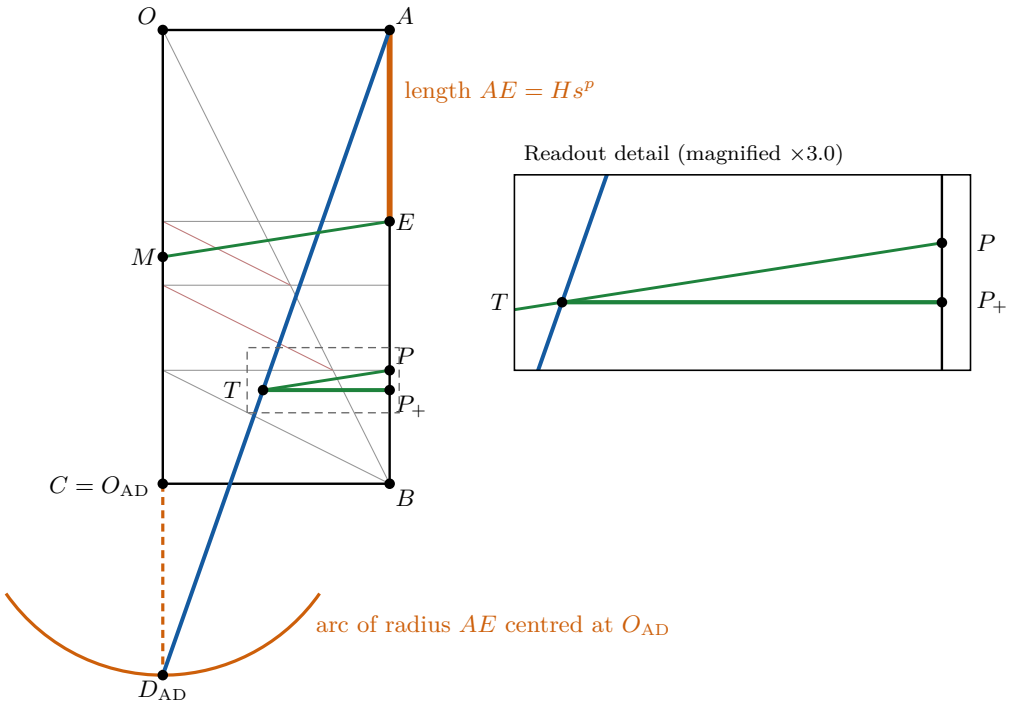



**Figure 8:** Pandrosion AD, order three, at the same state. The orange length $AE$ is transferred onto the prepared vertical through $O_{AD}$; the lower arc point determines the support $AD_{AD}$ (blue). Here $O_{AD} = C$.

(The line $\ell$ of this appendix is unrelated to the length $\ell$ of Figure 2.) Set $D_{proj} = Z_{proj}E \cap \ell$ and join $AD_{proj}$. Substitution in (2.3) gives the $\kappa$ of Table 3 and

$$T_{proj}(s) = s\,\frac{2p\big((2p-1)t+p+1\big)}{Q_{proj}(t)}, \qquad Q_{proj}(t) = (p+1)t^2 + 2(2p-1)(p+1)t + (2p-1)(p-1). \quad \text{(A.2)}$$

The direct-root correction is the [2/1] Padé approximant; the reciprocal-state factor displayed here is [1/2]. Direct differentiation gives

$$T'_{proj}(s) = -\frac{2p(p^2-1)(2p-1)(t-1)^3}{Q_{proj}(t)^2},$$

so the map has its global maximum $\alpha$ at $s = \alpha$. Also $T_{proj}(s)/s - 1 = (1-t)\big((p+1)t + 5p - 1\big)/Q_{proj}(t)$. Thus a first step lands at or below $\alpha$ and subsequent steps increase to $\alpha$; the order is exactly four. The earlier preprint gives further dynamics and the original triangle-chain realization [22].

# B The linear MB reference

MB is a baseline, not an accelerated method. Its support is the line $MB$, from the prepared point $M$ to the lower-right vertex $B$; it does not pass through $A$. Earlier versions called this construction MA: the name referred to the same lower-right vertex, which is $B$ in the labelling of this paper. The parallel to $ME$ through $P$ meets $MB$, and a horizontal returns the next state. For $s \neq 1$,

$$T_{MB}(s) = 1 - \frac{X-1}{X\,\Sigma_p(s)}, \qquad \Sigma_p(s) = \sum_{j=0}^{p-1} s^j.$$

For $X > 1$ this map is increasing and $T_{MB}(s) - s = (1 - Xs^p)/(X\Sigma_p(s))$, so it converges monotonically to $\alpha$ from every positive start, with the removable extension at $s = 1$. Its derivative at $\alpha$ is $1 - p\alpha^{p-1}/\Sigma_p(\alpha) \in (0, 1)$: convergence is linear.

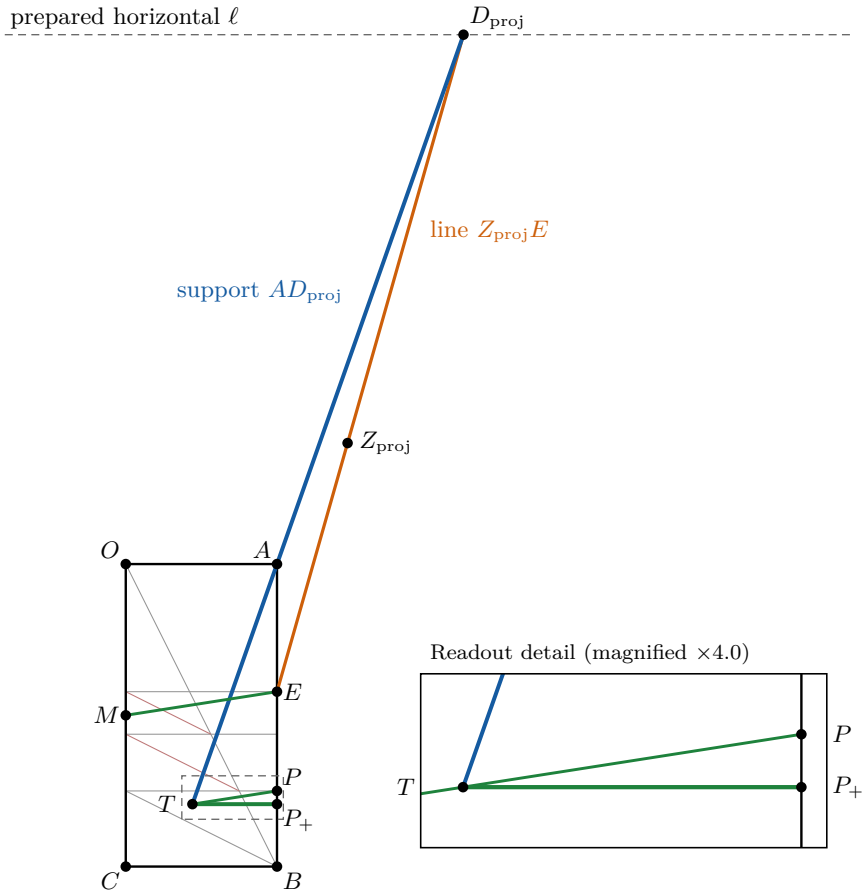



**Figure 9:** Projective AD, order four, at the same cubic state. The orange line $Z_{\mathrm{proj}}E$ meets the prepared horizontal $\ell$ at $D_{\mathrm{proj}}$; the blue support $AD_{\mathrm{proj}}$, extended below $A$, receives the green correction. The inset magnifies the dashed window and separates $P$, $T$ and $P_+$.

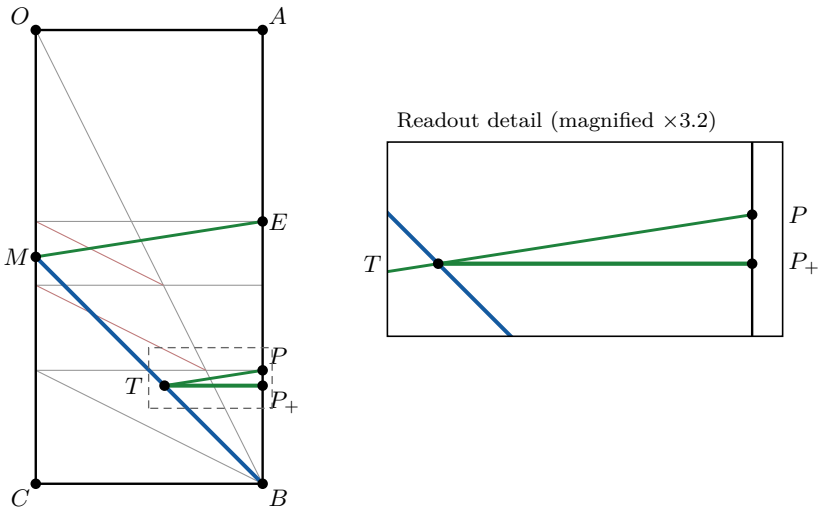



**Figure 10:** Pandrosion MB, the linear reference construction, at $p = 3$, $X = 2$, $s = 3/4$. Thin lines construct the power by similar triangles. The green parallel meets the blue support $MB$; the horizontal gives $P_+$. At $s = 1$ the geometric intersection is coincident despite the removable scalar extension.

# C Equivalence questions for the radical corrections

Whether the arc is a known formula "up to conjugacy" depends on the class of coordinate changes allowed. Let $\varphi$ denote the correction factor $\Phi_{\mathrm{arc}}(t) = (1+g)/(t+g)$ with $g = (p-1)q_5$. Eliminating the radical gives the quadratic relation

$$P_p(t,\varphi) := (p-1)^2 S(t)(\varphi-1)^2 - 12p\,(t\varphi-1)^2 = 0. \tag{C.1}$$

The explicit radical in (3.1) selects the branch; the polynomial alone loses sign information and has a double root at $t = 1$.

**Homographic changes.** For each real $p > 2$, $\Phi_{\mathrm{arc}}$ is not rational in $t$. Indeed $\mathrm{disc}_t\, S = 96p(p+1)$ and $S(0) = p-2 > 0$, so $S$ has two simple nonzero roots and is not a square in $\mathbb{C}(t)$; if the correction were rational, so would be $\sqrt{S(t)/(12p)} = (1-t\Phi_{\mathrm{arc}})/[(p-1)(\Phi_{\mathrm{arc}}-1)]$. Invertible homographies of the input or output preserve rationality. For integer $p \geq 3$, $S(y^p)$ also has only simple roots, so the state map $y\,\Phi_{\mathrm{arc}}(y^p)$ is not rational and cannot be Möbius-conjugate to a rational state map, even as a germ at $y = 1$. This state-map exclusion is asserted only for integer degrees.

**A specified quadratic normalization.** A diagonal type $(2,2,2)$ quadratic Hermite–Padé (Shafer) form for $f(t) = t^{-1/p}$ requires polynomials of degree at most two with $A(t)f^2 + B(t)f + C(t) = O((t-1)^8)$ [23, eqs. (1.4)–(1.6)]. Direct substitution into (C.1) gives instead, with $\xi = t-1$,

$$P_p\big(1+\xi, (1+\xi)^{-1/p}\big) = \frac{(p-2)(p-1)^2(p+1)(3p+1)}{60p^4}\,\xi^6 + O(\xi^7),$$

contact six, not eight. The coefficients of $P_p$ have no common factor and its discriminant in $\varphi$ is $48p(p-1)^2(t-1)^2S(t)$, so it is irreducible over $\mathbb{C}(t)$; any polynomial with the same degree bounds defining this branch is a constant multiple of $P_p$. This excludes that particular diagonal approximant in these coordinates, without excluding other algebraic families or transformed targets.

**Local analytic conjugacy.** Distinct formulas may share a local analytic normal form: Böttcher's theorem conjugates a superattracting germ $F(e) = ce^{\varrho} + O(e^{\varrho+1})$, $c \neq 0$, to its monomial normal form [24]. This supplies neither a finite incidence protocol nor a global domain or drawing inventory. The explicit construction and its proved dynamics are therefore distinct from a claim of a new local conjugacy class.

**The three-mean correction as a constrained quadratic approximant.** Put $\sigma = \sqrt{t} + 1/\sqrt{t}$, so that $w = \sigma^2 - 4$. Then

$$\frac{q_5}{\sqrt{t}} = \sqrt{1 + a_9(\sigma^2-4)}, \qquad \frac{q_M}{\sqrt{t}} = m\,\sigma + g - n\sqrt{1 + d\,(\sigma^2-4)},$$

and $y = q_M/\sqrt{t}$ satisfies $(y - m\sigma - g)^2 = n^2\big(1 + d(\sigma^2-4)\big)$, a quadratic relation whose coefficients have degrees $0, 1, 2$ in $\sigma$. In this variable the three-mean support is therefore a quadratic algebraic approximant of $q_*/\sqrt{t}$ at $\sigma = 2$ in the sense of [15], but not the Hermite–Padé approximant of its type: its discriminant is constrained to have no term of degree one in $\sigma$. The constraint is what keeps the radicand a quadratic polynomial in $t$, that is, one arc. The unconstrained form has one more free coefficient. For $p = 3$ it is

$$\frac{16}{33} - \frac{\sigma}{66} + \frac{1}{99}\sqrt{5\sigma^2 + 736\sigma + 1424} = \frac{q_*}{\sqrt{t}} + \frac{(\sigma-2)^5}{19131876} + O\big((\sigma-2)^6\big),$$

one order more than (5.9), where the error is $\frac{23}{354294}(\sigma-2)^4$; but multiplied by $t$ its radicand contains $\sqrt{t}$, so the corresponding support is a nested radical. This is an exact rational computation on the series at $p = 3$; the corresponding iteration has not been analysed.

# References

[1] Pappus of Alexandria. *Book III of the Mathematical Collection*. English translation by John B. Little, following Hultsch; College of the Holy Cross, Bookshelf 63, 2023. https://crossworks.holycross.edu/hc_books/63/.

[2] Mickaël Launay. Pandrosion et la duplication du cube. Micmaths, video presentation, 2024. https://www.youtube.com/watch?v=7T4neM660SM. Rectangle construction and correction, approximately 16:37–19:10.

[3] Alexei V. Sergeev and David Z. Goodson. Summation of asymptotic expansions of multiple-valued functions using algebraic approximants: application to anharmonic oscillators. *J. Phys. A: Math. Gen.* 31:4301–4317, 1998. https://avsergeev1.narod.ru/papers_37_iop_paper.pdf.

[4] Euclid. *Elements*, Book VI, Proposition 13. Online edition by David E. Joyce, Clark University. https://mathcs.clarku.edu/~djoyce/elements/bookVI/propVI13.html. Accessed 17 October 2026.

[5] Ivan Besevic. Real exponents: geometric subdivision. Pandrosion Geometry Workshop, companion interactive construction, 2026. https://ivan-fr.github.io/pandrosion/gallery/geometric-subdivision.html. Local source snapshot included with the V26-S supplement.

[6] NIST Digital Library of Mathematical Functions. Section 3.11(iv): Padé approximations. https://dlmf.nist.gov/3.11#iv. Accessed 17 October 2026.

[7] George A. Baker, Jr. and Peter Graves-Morris. *Padé Approximants*, 2nd ed. Encyclopedia of Mathematics and its Applications 59, Cambridge University Press, 1996. doi:10.1017/CBO9780511530074. In particular Section 1.5, Theorems 1.5.2–1.5.3, on argument and value homographic invariance.

[8] J. F. Traub. On a class of iteration formulas and some historical notes. *Comm. ACM* 4(6):276–278, 1961. doi:10.1145/366573.366606.

[9] J. F. Traub. *Iterative Methods for the Solution of Equations*. Prentice-Hall, 1964.

[10] A. M. Ostrowski. *Solution of Equations and Systems of Equations*. Academic Press, New York, 1960.

[11] Walter Gander. On Halley's iteration method. *Amer. Math. Monthly* 92(2):131–134, 1985. doi:10.2307/2322644.

[12] T. R. Scavo and J. B. Thoo. On the geometry of Halley's method. *Amer. Math. Monthly* 102(5):417–426, 1995. doi:10.2307/2975033.

[13] A. Melman. Geometry and convergence of Euler's and Halley's methods. *SIAM Review* 39(4):728–735, 1997. doi:10.1137/S0036144595301140.

[14] S. Amat, S. Busquier and J. M. Gutiérrez. Geometric constructions of iterative functions to solve nonlinear equations. *J. Comput. Appl. Math.* 157(1):197–205, 2003. doi:10.1016/S0377-0427(03)00420-5.

[15] R. E. Shafer. On quadratic approximation. *SIAM J. Numer. Anal.* 11(2):447–460, 1974. doi:10.1137/0711037.

[16] Émile Lemoine. *Géométrographie ou Art des constructions géométriques*. Scientia 18, C. Naud, Paris, 1902. https://catalogue.bnf.fr/ark:/12148/cb36049032t.

[17] Maurice d'Ocagne. *Esquisse d'ensemble de la nomographie*. Mémorial des sciences mathématiques 4, Gauthier-Villars, 1925. https://www.numdam.org/item/MSM_1925__4__1_0/.

[18] Leonardo de Moura and Sebastian Ullrich. The Lean 4 theorem prover and programming language. In *CADE 28*, LNCS 12699, pages 625–635. Springer, 2021. doi:10.1007/978-3-030-79876-5_37.

[19] The mathlib Community. The Lean mathematical library. In *CPP 2020*, pages 367–381. ACM, 2020. doi:10.1145/3372885.3373824. https://leanprover-community.github.io/papers/mathlib-paper.pdf.

[20] Ivan Besevic. Nested-radical Pandrosion support: derivation, geometric example and Lean convergence certificates. Source bundle accompanying *Geometric Root Calculators*, V27-NR, 18 October 2026. Includes `NestedRadicalCubic`, `NestedRadicalRealCertificate`, `NestedRadicalReal`, `NestedRadicalAllDegrees`, audit scripts, source hashes and numerical checks.

[21] Ivan Besevic. Geometric subdivision and Padé readout: supplementary source and verification records. Source bundle accompanying *Geometric Root Calculators*, V26-S, 2026. Includes `GeometricSubdivision.lean`, its retained axiom audit and the independent subdivision verifier.

[22] Ivan Besevic. Reciprocal root geometry, version 20. Research preprint, 2026. https://github.com/ivan-fr/pandrosion/tree/main/paper/reciprocal_geometry_v20.

[23] Stan Cabay and George Labahn. A fast, reliable algorithm for calculating Padé–Hermite forms. Technical Report CS-89-09, University of Waterloo, 1989. https://cs.uwaterloo.ca/research/tr/1989/CS-89-09.pdf. Equations (1.4)–(1.6), printed page 1, PDF page 5.

[24] Xavier Buff, Adam L. Epstein and Sarah Koch. Böttcher coordinates, 2011. https://arxiv.org/abs/1104.2981. Introduction: the classical one-variable theorem.

[25] B. C. Carlson. The logarithmic mean. *Amer. Math. Monthly* 79:615–618, 1972.

[26] Kenneth B. Stolarsky. Generalizations of the logarithmic mean. *Math. Mag.* 48(2):87–92, 1975. doi:10.2307/2689825.

[27] François Dubeau. Newton's method and high-order algorithms for the $n$th root computation. *J. Comput. Appl. Math.* 224:66–76, 2009. doi:10.1016/j.cam.2008.04.014.

[28] Ivan Besevic. Complex geometric root calculators, version C3. Research preprint, companion to this paper, 13 November 2026.